

Amplitude- and frequency-dependent nonlinearities in the presence of thermally-induced transitions in the Preisach model of acoustic hysteresis

V. Gusev* and V. Tournat

Université du Maine, 712085 Le Mans, France

(Received 16 August 2004; revised manuscript received 24 February 2005; published 2 August 2005)

Contribution of hysteretic mechanical elements to the stress/strain relationship of microinhomogeneous material is analyzed within the framework of a model where the transitions between the different mechanical states of the individual elements in addition to acoustic loading can be induced by thermal fluctuations. The model provides explanation for the dependence of the type and order of the acoustic nonlinearity on the wave amplitude observed in experiments with microinhomogeneous materials, where, with increasing wave amplitude, transition from behavior characterized by the dominance of the quasilinear nonlinearity to another characterized by the dominance of hysteretic quadratic nonlinearity takes place. Analytical evaluation of the model for the acoustic hysteresis is shown to confirm the expectation that thermal relaxation effects are capable of inducing dispersion in both the linear and nonlinear acoustic properties of the material.

DOI: [10.1103/PhysRevB.72.054104](https://doi.org/10.1103/PhysRevB.72.054104)

PACS number(s): 62.65.+k, 62.40.+i, 62.30.+d, 43.25.+y

I. INTRODUCTION

Due to the high acoustic nonlinearity of microinhomogeneous materials such as rocks, polycrystalline metals, and ceramics, for example, the methods of the nonlinear acoustics have become increasingly applied for their nondestructive characterization.¹⁻⁴ Currently there exists a consensus, that mechanical properties of these materials are dominated by the hysteretic nonlinearity, as opposed to the nonlinearity of the interatomic interactions and the kinematic nonlinearity.^{5,6} Hysteretic nonlinearity is understood phenomenologically in terms of the nonlinear motion of the mesoscopic mechanical elements such as dislocations, intergrain contacts, or defects, for example, with the dimensions exceeding interatomic distances but significantly smaller than the acoustic wavelength.^{1,3} As the mathematical tools for the description of nonlinearity hysteresis, different modifications of the Granato-Lucke theory for the acoustically induced motion of the dislocations^{7,8} or the Preisach-Mayergoyz model of the hysteresis⁹⁻¹³ can be applied. In their simplest formulations both approaches predict that the dominant hysteretic nonlinearity is quadratic (i.e., even) in acoustic wave amplitude, but that nonlinearity acts as an odd type nonlinearity in its physical manifestations.^{1-4,14-17} For example, the harmonics excited in the propagation of an initially sinusoidal wave are at short distances quadratic in the initial wave amplitude; however the quadratic nonlinearity yields only odd harmonics in the experimentally observed Fourier decomposition of the wave.^{14,15} Existing models explain what is perhaps the best known and the most common manifestation of the hysteretic quadratic nonlinearity which is the shift of the resonance frequency of a solid microinhomogeneous bar proportional to the wave amplitude in the bar.¹⁻⁴

The theoretical analysis presented below was initially motivated by a recent communication¹⁸ reporting that at very low acoustic strain amplitudes the shift of the resonance in rock rods is not linear in wave amplitude and that there exists a critical strain amplitude $O(10^{-6})$ at frequencies as low as 0.5–3 kHz where the transition to common linear depen-

dence takes place with increasing wave amplitude. Surprisingly a similar transition has been reported in classical experiments on single crystal metals with dislocations at a strain level $O(10^{-7})$ at a frequency of 39 kHz over 50 years ago,¹⁹ but which appears to be without citation in the literature. A recent communication (Ref. 20), reported the same phenomenon in polycrystalline metal at strain levels of 2.5×10^{-6} – 5×10^{-6} at frequencies 2.7–13.5 kHz. Consequently a low amplitude threshold for the manifestation of the frequency shift linear in wave amplitude (typical to the Preisach-Mayergoyz model of hysteresis) appears to be well documented in a number of mesoscopic materials, while the model itself does not predict this threshold.

In order to resolve this contradiction we propose here to take into account that hysteresis is always a dynamic phenomenon. If the thermal fluctuations, pushing the system to a unique equilibrium state, are taken into account in the description of the mesoscopic elements, then there will be no hysteresis in the static limit. The hysteresis will appear in quasistatics at such frequencies where the thermal fluctuations have insufficient time to put the system in its absolute minimum of free energy during the wave period and the system can be found in a local minimum, which constitutes a metastable state. Consequently, the nonlinear mesoscopic mechanical elements, in reality, are nonhysteretic in the static limit and hysteretic only in their dynamic behavior. Then there are certainly sufficiently low frequencies where the nonlinear behavior is predominantly nonhysteretic rather than hysteretic, and the transition from one type of nonlinearity to another can be achieved by increasing the frequency. With this statement in hand a possible explanation for the observed low-amplitude threshold for the observation of the hysteretic quadratic nonlinearity might be provided by a proof that the transition in the behavior of mesoscopic elements to one described the PM model can be initiated not only by increasing the acoustic frequency but also by increasing the acoustic amplitude. It is shown here that the behavior of this transition with increasing wave amplitude can be described, in particular, by the Preisach-Arrhenius

model for the acoustic response of microinhomogeneous (mesoscopic) materials.

In the present publication we analyze the dependence of the elastic acoustic nonlinearity on acoustic wave amplitude and frequency, as well as the frequency-dependent nonlinear sound decrement within the framework of the Preisach-Arrhenius model for hysteresis. We note parenthetically here that the Preisach (Preisach-Mayergoyz) formalism^{9–13} attributes hysteresis in the nonlinear stress/strain relationship to superposed behavior of individual noninteracting bistable (two-level) hysteretic mechanical units, sometimes referred to as hysterons.^{12,21–23} The transitions between two possible states, i.e., energy levels, are assumed to take place instantaneously and exactly at some critical levels of varying stress (strain). For different individual mechanical elements the levels are different. This model of the hysteretic nonlinearity is essentially dispersionless, that is frequency-independent, because there are no characteristic scales of either time or length in the model. The Preisach-Arrhenius model applied, in particular, for the description of thermally activated relaxation, or “aftereffect,” in magnetic materials^{13,21–25} takes into account that the transitions between the energy levels of the system can be thermally activated and that the probability of the transition is controlled by the Boltzmann factor $\exp(-\Delta E/k_B T)$, where ΔE is the energy barrier between the levels, or some activation energy, k_B is the Boltzmann constant, and T is the absolute temperature. The thermally controlled transition is not instantaneous, rather, there is a characteristic time scale for each individual mechanical element that can be estimated by $\tau_0 \exp(\Delta E/k_B T)$ as defined by the Arrhenius formula for the transition time, where τ_0 is some characteristic attempt time associated with the jump (Barkhausen jump^{13,24}) between the energy levels. Consequently dispersion in the acoustic nonlinearity is expected in the Preisach-Arrhenius model. The acoustic wave influences the system through the modulation of the energy barrier ΔE between the energy levels. Thus the acoustic wave influences thermally activated relaxation processes in the system making them amplitude-dependent. Qualitatively speaking, the Preisach-Arrhenius model describes nonlinear temperature-dependent relaxation of the nonlinear hysteretic mechanical elements. Consequently it might be expected that the nonlinearity of the system is due not only to the intrinsic nonlinearity of the bistable hysteretic elements but also due to the nonlinearity of the relaxation process.

It should be mentioned that some time ago the possibility of thermal activation of the unpinning process had been introduced in the theory of acoustic damping due to dislocation motion.^{26,27} However, to the best of our knowledge, no analysis of the dispersion of the acoustic properties and their detailed dependence on the acoustic wave amplitude was undertaken.

The text is organized as follows: In Sec. II we present the derivation of the stress/strain relationship for an arbitrary strain loading history within the framework of the Preisach-Arrhenius model. Sections III–VI include the results of analytical evaluation of the elastic and inelastic linear and nonlinear properties of the model as a function of the sinusoidal or quasiperiodic strain amplitude and frequency. Asymptotic analytical results have been obtained in the lim-

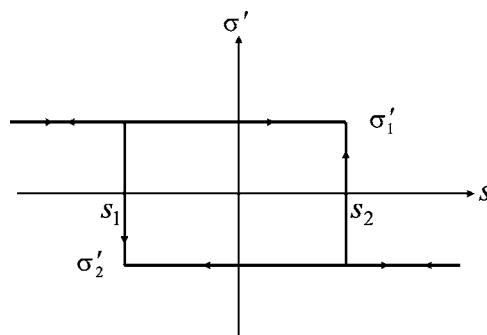


FIG. 1. Contribution σ' of an individual mechanical element to stress in the framework of the Preisach-Mayergoyz model. Arrow-heads indicate direction of strain variation in time.

its of low and high acoustic frequencies, and in the limit of weak amplitude and high amplitude acoustic excitation. Discussion of the theory is presented in Sec. VII followed by the conclusions in Sec. VIII. The goal of our research was to analyze theoretically various possible cases related to characteristic parameters of the model rather than to seek quantitative agreement with real experimental situations.

II. PREISACH-ARRHENIUS MODEL FOR ACOUSTIC RESPONSE OF MICROINHOMOGENEOUS MEDIA

There exists a consensus that microinhomogeneous materials may contain some mechanical elements which are mesoscopic (with the dimensions exceeding the atomic scale but significantly smaller than acoustic wavelength) and hysteretic (like reversible Griffith cracks¹⁰ or contacts with adhesion,²⁸ for example). The hysteresis in the behavior of an individual mechanical element might be imagined in the simplest way as being related to possibility for the element to be in different states (or configurations) under the same mechanical loading. In which state actually might be found the mechanical element depends on the acoustic loading history. Both in the Preisach-Mayergoyz (PM) (Refs. 9–13) and the Preisach-Arrhenius (PA) (Refs. 13 and 21–25) models it is assumed that the mechanical elements have two states (two level systems) and that the contribution σ' of an element to stress depends on its state. This is a phenomenological description in which the multilevel multistable free-energy structure (of interacting between themselves and with the matrix mechanical elements) is decomposed into many two-level bistable contributions.¹³ In the PM theory the transition of an element from state 1 to state 2 takes place with increasing strain s when $\partial s / \partial t > 0$, $s = s_2$, while the inverse transition with decreasing strain takes place when $\partial s / \partial t < 0$, $s = s_1 < s_2$ (Fig. 1). It is the difference between the critical switching strains s_2 and s_1 ($s_2 \neq s_1$) that gives opportunity to call an element hysteretic.

We are using a strain controlled hysteretic element (Fig. 1), but not a stress controlled element. The most important point here, in our opinion, is that in nonlinear acoustics both approaches are absolutely equivalent from the physics point of view. When we are analyzing weak (acoustic) loading of a material the nonlinearity of the material (i.e., the deviation

from the Hooke's law in the diapason of load variation) is weak. The relation between stress and strain in acoustic wave is in the leading (dominant) order linear and controlled by the linear elastic modulus E . In acoustic experiments the wave controls local load on the mechanical system both in terms of stress and in terms of strain (which are just related via the elastic modulus). To analyze the modification of an element by the acoustic strain, it is sufficient to evaluate the additional to prescribed by the Hooke's law strain-induced variations of stress (as thermodynamically conjugated variable to strain) and to neglect the accompanying strain-induced strain variations, thus considering the element as being strain controlled. To analyze the modifications of an element by acoustic stress it is sufficient to evaluate the additional to prescribed by the Hooke's law stress-induced variations in strain (as thermodynamically conjugated variable to stress) and to neglect the accompanying stress-induced stress variations, thus considering the element as being stress controlled. We prefer to analyze strain controlled mechanical elements, because then we directly get the additional (due to hysteretic elements) contribution to stresses and these are stress gradients that are (in accordance with elasticity theory) providing acceleration of a medium. It has been demonstrated that both strain controlled and stress controlled hysteresons provide the same functional form of non-linearity in acoustics.¹⁶

If the notation $f(s_1, s_2)$ is introduced for the distribution function of the elements in the plane (s_2, s_1) (PM plane) then the contribution of all the elements to the stress can be presented as

$$\sigma = \int_{-\infty}^{s_2} ds_1 \int_{s_1}^{\infty} ds_2 \sigma'(s_1, s_2, s) f(s_1, s_2). \quad (1)$$

Here $f(s_1, s_2) ds_1 ds_2$ is the number of elements with critical strains belonging to the intervals $(s_1, s_1 + ds_1)$ and $(s_2, s_2 + ds_2)$ of the PM plane (s_2, s_1) . Due to the assumed condition $s_2 > s_1$ the integration in the PM plane is in the half-space at the right of the diagonal $s_2 = s_1$ (Fig. 2). The arguments of the function $\sigma'(s_1, s_2, s)$ indicate that in general the contribution of an element to the total stress depends on its position at the PM plane and the loading history as it is presented in Fig. 1. Important feature of the PM model is that hysteresis in the mechanical behavior of the individual elements exists independently of the strain rate magnitude (there is only the dependence on the sign of the strain rate). It is assumed that transitions at critical levels s_2 and s_1 are instantaneous. It is assumed that the transition $1 \Rightarrow 2$ will always happen when strain s ($\partial s / \partial t > 0$) exceeds s_2 independently of how fast s returns back to the region $s < s_2$ after that. From a physics point of view in the PM model it is the acoustic loading that not only creates the conditions for the transition but also induces the change of the state. In the theory of magnetism the Preisach-Mayergoyz model is considered as a zero-temperature model of rate-independent hysteresis.¹³

The physical nature of $\sigma'(s_1, s_2, s)$ behavior in the Preisach-Arrhenius model is very different. It is not only the acoustic field, which can itself transfer the mechanical elements between the states 1 and 2. These are also thermal

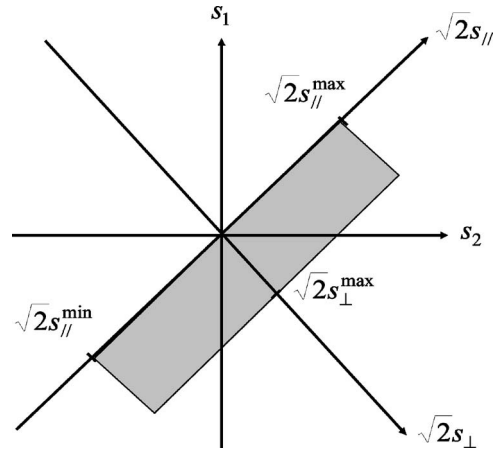


FIG. 2. Presentation of mechanical element distribution at Preisach-Mayergoyz plane (s_2, s_1) , where s_2 and s_1 are the critical strain values for switching the elements between the levels. In general the elements can occupy the complete half-plane $s_2 > s_1$ ($s_{\perp} = (s_2 - s_1)/2 > 0$). A distribution, limited in the PM plane by $s_{\perp} \leq s_{\perp}^{\max}$ and $s_{\parallel}^{\min} \leq s_{\parallel} = (s_2 + s_1)/2 \leq s_{\parallel}^{\max}$, is presented in gray as an example.

fluctuations that statistically can always cause the transitions. Thus in the PA model the transition from the state 1 to the state 2, for example, is not restricted to $s = s_2$ ($\partial s / \partial t > 0$) and instantaneous, but is possible for all s although with a finite probability depending on the level of s relative to s_2 . Once the temperature is introduced the element can overcome the energy barrier by thermal activation at lower strains (stresses) as long as there is a second (local) energy minimum in which to jump. Qualitatively speaking thermal fluctuations accelerate the transitions below the critical level of strain s_2 .

In the Arrhenius model of thermally initiated transitions, the transition time τ_{12} from level 1 to level 2 is equal to

$$\tau_{12} = \tau_0 \exp[d(s_2 - s)/k_B T], \quad (2)$$

where τ_0 is the so-called attempt time,^{13,21,26,29} d is the parameter describing the variation of energy difference between the states 1 and 2 with strain (deformation potential), and $k_B T$ is the characteristic thermal energy. There are few restrictions on the applicability of the model in Eq. (2). First, the model in Eq. (2) is theoretically established for the situation when two free energy minima exist simultaneously^{13,21} i.e., in the strain interval $s_1 \leq s \leq s_2$. However, by extending the application of the model in Eq. (2) to $s \geq s_2$, for example, one could try to qualitatively account for the fact that the transition between two configurations even in the absence of the potential barrier between them could have taken some time. Note that in accordance with Eq. (2) the transition time τ_{12} diminishes exponentially fast below the value of τ_0 with increasing strain when strain passes the critical level s_2 . So the extension of Eq. (2) to $s \geq s_2$ insures that in the dynamic regime of loading the transition to a second single energy minimum (stable state) will take place after the disappearance of the first (metastable) state. Otherwise Eq. (2) can be viewed as a smooth approximation for the theoretical τ_{12} ,

which is equal to infinity when $s < s_1$, is described by Eq. (2) when $s_1 \leq s \leq s_2$, and is equal to zero when $s \geq s_2$. Third, in the following it will be considered that the deformation potential is the same for all the Preisach units (d does not depend on s_1 and s_2). This approximation correlates with the fundamental requirements for validity of Preisach approach to description of the hysteretic systems, i.e., with the possibility of the decomposition of the free energy of the system into elementary noninteracting bistable contributions (even if we do not know why this decomposition is possible^{13...}). It is important that the dependence of the ‘‘amplitudes’’ of the individual Preisach units contribution to stress [$\sigma'(s_1, s_2, s)$ in Eq. (1)] on s_1 and s_2 can be incorporated in their distribution function $f(s_1, s_2)$. See for the details the discussion following Eq. (9) below. Thus the Preisach decomposition into the equal amplitude hysterons (with equal $\sigma'_1 - \sigma'_2$ in Fig. 1 for all the elements) is possible. The deformation potentials for the units of equal amplitude are equal (see, for comparison, Fig. 13.1 from Ref. 13).

Similarly to τ_{12} the time τ_{21} of the inverse transition is

$$\tau_{21} = \tau_0 \exp[d(s - s_1)/k_B T]. \quad (3)$$

The transition times τ_{12} and τ_{21} control the probabilities W_1 and W_2 to find the element in the states 1 and 2, respectively,

$$\partial W_1 / \partial t = -W_1 / \tau_{12} + W_2 / \tau_{21},$$

$$\partial W_2 / \partial t = W_1 / \tau_{12} - W_2 / \tau_{21}, \quad W_1 + W_2 = 1. \quad (4)$$

These equations are sufficient to describe the dynamics of stress in response to acoustical loading. Actually the average level of $\sigma'(s_1, s_2, s)$ in the absence of the acoustic wave does not contribute to dynamic stress in Eq. (1). Thus it is useful to evaluate the variations of $\sigma'(s_1, s_2, s)$ relative to the average level $(\sigma'_1 + \sigma'_2)/2$, where σ'_1 and σ'_2 are the contributions to stress when the element is in the positions 1 and 2, respectively. Then the contributions of the states 1 and 2 to stress that can be modified by acoustic excitation are described as $(\sigma'_1 - \sigma'_2)/2 \equiv \Delta\sigma'(s_1, s_2)$ and $(\sigma'_2 - \sigma'_1)/2 \equiv -\Delta\sigma'(s_1, s_2)$, respectively. Taking into account the probabilities to find the element in the corresponding states, the strain dependent contribution $\sigma''(s_1, s_2, s)$ to $\sigma'(s_1, s_2, s)$ can be presented as

$$\begin{aligned} \sigma''(s_1, s_2, s) &= -\Delta\sigma'(s_1, s_2)W_2 + \Delta\sigma'(s_1, s_2)W_1 = \Delta\sigma'(s_1, s_2) \\ &\times (W_1 - W_2) \equiv \Delta\sigma'(s_1, s_2)Q. \end{aligned} \quad (5)$$

The relations (4) lead to a single equation describing the dynamics of the introduced in Eq. (5) function Q , which characterizes the asymmetry of the element distribution between the two levels,

$$\partial Q / \partial t + (1/\tau_{21} + 1/\tau_{12})Q = (1/\tau_{21} - 1/\tau_{12}). \quad (6)$$

An evident but important conclusion based on Eq. (6) is the absence of the hysteresis in the contribution of an element to stress under the static conditions. For $\partial/\partial t \rightarrow 0$ (zero frequency of the acoustic action) the solution of Eq. (6) is

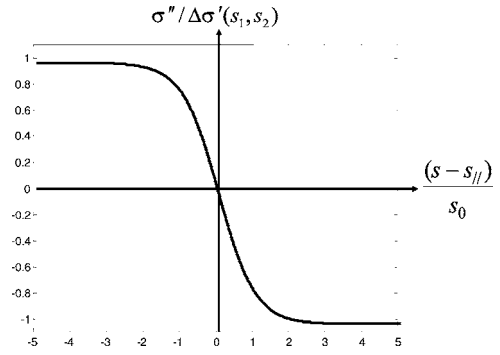


FIG. 3. Contribution σ'' of an individual mechanical element to stress in the framework of the Preisach-Arrhenius model in the case of infinitely low frequency of acoustic action. The element behaves in response to strain variation as a two-level but a nonhysteretic unit.

$$Q_0 = -\tanh \left[d \left(s - \frac{s_1 + s_2}{2} \right) / k_B T \right]. \quad (7)$$

Thus, in contrast to the PM model the hysteresis in the PA model is a dynamic phenomenon due to the finite rate of acoustic loading (compare the solutions for σ' in Fig. 1 and in Fig. 3).

For the following analysis the characteristic strain $s_0 = k_B T / d$, which provides a scale for the amplitude of acoustic loading necessary for significant (e times) modification of the relaxation times τ_{12} and τ_{21} , is introduced. All the strains are normalized to this level ($s/s_0 \equiv s$, $s_{1,2}/s_0 \equiv s_{1,2}$). Two new variables $s_{||} = (s_2 + s_1)/2$ and $s_{\perp} = (s_2 - s_1)/2$ are then introduced. The modulus of the first one characterizes the average acoustic strain necessary for initiation the transitions in the element (s_1, s_2) of the PM space. The second one characterizes the separation of forward and backward transitions. Qualitatively speaking $|s_{||}|$ characterizes the average energy of the mechanical element (from the acoustics point of view) while s_{\perp} characterizes the separation of the energy levels 1 and 2 in the absence of the acoustic loading. On the other hand $s_{||}$ and s_{\perp} have a clear geometrical sense being proportional in the PM plane to the coordinates measured along the diagonal $s_2 = s_1$ and perpendicularly to the diagonal, respectively^{13,30,31} (Fig. 2).

Just to give the readers an idea of a plausible value for the scale s_0 , it is worth to present here the estimates of s_0 , obtained later in Sec. VII via the comparison of the predictions of the developed theory with some available experimental data. It is estimated that at room temperatures $s_0 \propto (1-2) \times 10^{-8}$ in single crystal metals (where the plausible micromechanical elements are dislocations) and $s_0 \propto (3-6) \times 10^{-8}$ in rocks.

Note, that as far as $T \neq 0$ (corresponding to experimental reality) there is no problems in normalization of strains to $s_0 = k_B T / d \neq 0$. The normalization to s_0 has no sense only in the theoretical limiting point $T=0$, where however the Preisach-Mayergoyz model of the rate-independent zero-temperature hysteresis can be used just from the beginning. The answer to the question, why the PM model of rate-

independent zero-temperature hysteresis describes successfully some experiments conducted at finite temperatures $T \neq 0$ and under what conditions it is possible to use the PM model, is given later in Sec. VI. There it is demonstrated that these are conditions simultaneously on the normalized acoustic wave amplitude ($s_A/s_0 \propto 1/T$) and the normalized acoustic frequency ($F = \tau_0/T_A$).

In the introduced notations Eq. (6) takes the form

$$\begin{aligned} \partial Q / \partial \theta + (2/F) \exp(-s_{\perp}) \cosh(s(\theta) - s_{\parallel}) Q \\ = - (2/F) \exp(-s_{\perp}) \sinh(s(\theta) - s_{\parallel}). \end{aligned} \quad (8)$$

Here the time is normalized to the period T_A of acoustic loading $\theta = t/T_A$, and the parameter $F = \tau_0/T_A$ is the normalized frequency of the acoustic action. This particular normalization is chosen, because in the following the analysis will be concentrated on the case of a sinusoidal loading, characterised by a single time-scale T_A . The integral relation (1) for the evaluation of the stress becomes

$$\sigma = s_0^2 \int_0^{\infty} ds_{\perp} \int_{-\infty}^{\infty} ds_{\parallel} \Delta \sigma'(s_{\perp}, s_{\parallel}) f(s_{\perp}, s_{\parallel}) Q(s_{\perp}, s_{\parallel}, s). \quad (9)$$

The formulas (8) and (9) with an appropriate modeling of the distributions $\Delta \sigma'(s_{\perp}, s_{\parallel})$ and $f(s_{\perp}, s_{\parallel})$ are sufficient for the description of the acoustic response of materials in the frame of the PA model. It is clear that the analysis should be first fulfilled for the simplest model of $\Delta \sigma'(s_{\perp}, s_{\parallel})$ and $f(s_{\perp}, s_{\parallel})$ variation in the PM plane (s_{\perp}, s_{\parallel}). For this purpose the product $\Delta \sigma'(s_{\perp}, s_{\parallel}) f(s_{\perp}, s_{\parallel})$ will be characterized by its characteristic value $(\Delta \sigma' f)_0$ and the extent of the elements distribution in the PM plane will be assumed limited by the boundaries $0 \leq s_{\perp} \leq s_{\perp}^{\max}$, $s_{\parallel}^{\min} \leq s_{\parallel} \leq s_{\parallel}^{\max}$ ($s_{\parallel}^{\min} < 0$, $s_{\parallel}^{\max} > 0$) (Fig. 2). Under these assumptions Eq. (9) simplifies

$$\sigma = s_0^2 (\Delta \sigma' f)_0 \int_0^{s_{\perp}^{\max}} ds_{\perp} \int_{-|s_{\parallel}^{\min}|}^{s_{\parallel}^{\max}} ds_{\parallel} Q(s_{\perp}, s_{\parallel}, s(t)). \quad (10)$$

Note that later the influence of the deviation of $\Delta \sigma'(s_{\perp}, s_{\parallel}) f(s_{\perp}, s_{\parallel})$ distribution from the one accepted here will be discussed (see Sec. VII). It is worth mentioning that the assumption $\Delta \sigma'(s_{\perp}, s_{\parallel}) f(s_{\perp}, s_{\parallel}) \approx \text{const}$ is rather common in applications of the Preisach-Mayergoyz model to acoustics, because only a small area of the PM plane with the dimensions $\propto s_A s_A / 2$ (where s_A is the amplitude of the acoustic wave) interacts with sound in the PM model. In this case the details of the $\Delta \sigma' f$ distribution outside this small area plays no role. In the Preisach-Arrhenius model the situation is different because acoustic wave perturbs the relaxation of all the elements of the PM plane and in principle the precise form of the distribution of the elements in the complete half plane should be known for the analysis of Eq. (9). However, from the physical considerations both the elastic energies of micromechanical elements ($\propto |s_{\parallel}|$) and the energy differences between the levels ($\propto |s_{\perp}|$) are limited from above. In other words the distribution $f(s_{\perp}, s_{\parallel})$ is in reality localized near the diagonal $s_1 = -s_2$ and simultaneously near the diagonal $s_1 = s_2$ ($\Delta \sigma' f$ diminishes both when $|s_{\parallel}| \rightarrow \infty$ and when $s_{\perp} \rightarrow \infty$). The latter conclusion is confirmed by the processing of the available experimental data.³⁴ Surely, the description of the

real distribution function $f(s_{\perp}, s_{\parallel})$ could require the introduction of the multiple scales both along the s_{\parallel} axis and along the s_{\perp} axis to account for a possible complicated relief of $f(s_{\perp}, s_{\parallel})$. However, in the first simplest analysis of the influence of the elements localization on the acoustic properties it looks reasonable to neglect a possible fine structure of $f(s_{\perp}, s_{\parallel})$ and just to account for the distribution localization by introducing a minimum number of the parameters. Thus we naturally arrive to the simplest model in Fig. 2, where s_{\perp}^{\max} and $s_{\parallel}^{\max} \propto |s_{\parallel}^{\min}|$ characterize the localization of the element distribution in the PM plane. The quantitative influence of the introduced parameters s_{\perp}^{\max} and $s_{\parallel}^{\max} \propto |s_{\parallel}^{\min}|$ on the acoustic response will be clear from the asymptotic analysis developed in Sec. III–V later. However, just now it is worth presenting the following qualitative arguments. From the structure of Eq. (8) it can be concluded that the characteristic relaxation cyclic frequency (i.e., the inverse relaxation time) for the function Q in the case of weak acoustic loading ($s \rightarrow 0$) can be estimated [from the coefficient in front of Q in the left-hand side of Eq. (8)] as

$$\omega_0 = (2/\tau_0) \exp(-s_{\perp}) \cosh(s_{\parallel}). \quad (11)$$

Consequently the boundaries of the elements distribution in the PM plane control the lowest [$\omega_L = (2/\tau_0) \exp(-s_{\perp}^{\max})$] and the highest [$\omega_H = (2/\tau_0) \cosh(s_{\parallel}^{\max})$] relaxation frequencies of the elements in the system. Here and in the following we consider for compactness that $s_{\parallel}^{\max} \propto |s_{\parallel}^{\min}|$. In accordance with Eq. (11) the relaxation frequency is lower for the elements with larger separation of the levels ($\partial \omega_0 / \partial s_{\perp} < 0$) and is higher for the elements with higher average energy of the levels ($\partial \omega_0 / \partial |s_{\parallel}| > 0$). In the PM plane the relaxation frequency of the elements diminishes with the deviation from the diagonal $s_{\perp} = 0$ and increase in both directions along the diagonal. Using the derived ω_L and ω_H it is possible to predict that the PA system will definitely reply to weak acoustic loading as a quasiequilibrium one if $2\pi/T \ll \omega_L$ [$\pi F \ll \exp(-s_{\perp}^{\max})$] and as a quasifrozen one if $2\pi/T \gg \omega_H$ [$\pi F \gg \cosh(s_{\parallel}^{\max})$]. In the former case the relaxation frequencies of all the elements are higher than the frequency of the acoustic excitation and the element state follows the acoustic loading with a very short delay (quasistatically). In the latter case the unperturbed by sound relaxation frequency of all the elements are lower than the frequency of the acoustic excitation and the elements have not enough time to change the state (they are quasifrozen).

It is worth mentioning here that in the most of the current physical theories it is accepted that the inverse attempt time (attempt frequency) $1/\tau_0$ is poorly known¹³ and is difficult to estimate. In addition, strictly speaking, it is not a constant. In particular, it depends on temperature. However the dependencies on other parameters are usually assumed to be of minor importance in comparison with strong exponential dependence, which is present in Eq. (2) and in Eq. (3). Values of $1/\tau_0$ in the range from 10^8 to 10^{12} Hz may be expected.^{13,27,29} They are expected to be related to the spectrum of phonons (vibrations) in the system. Consequently the nonequilibrium response of the Preisach-Arrhenius system at acoustic and even ultrasonic frequencies (rather than at hy-

personic frequencies in the range 10^9 – 10^{12} Hz) might be expected if there are elements with $\exp(-s_{\perp}) \ll 1$. Because of this in the following (and, particularly, in the presentation of the asymptotic results in Sec. III–V) it will be assumed that the inequality

$$\exp(-s_{\perp}^{\max}) \ll 1 \quad (12)$$

holds. That is at least $s_{\perp}^{\max} \geq 4$. The analysis demonstrates that the conditions on $s_{\parallel}^{\max} \propto |s_{\parallel}^{\min}|$ could be important only for hypersonics. In the following for the generality it will be assumed that

$$\exp(s_{\parallel}^{\max}) \propto \exp(|s_{\parallel}^{\min}|) \gg 1. \quad (13)$$

Under the conditions (12) and (13) the relation (11) predicts the existence of three well-separated frequencies in the system $\omega_0(s_{\perp}=s_{\perp}^{\max}, s_{\parallel}=0) = (2/\tau_0)\exp(-s_{\perp}^{\max})$, $\omega_0(s_{\perp}=0, s_{\parallel}=0) = (2/\tau_0) \ll \omega_0(s_{\perp}=0, s_{\parallel} \approx s_{\parallel}^{\max} \propto |s_{\parallel}^{\min}|) = (1/\tau_0)\exp(s_{\parallel}^{\max})$. As a consequence it is expected that system response to low-amplitude acoustic loading might have different behavior in the following four frequency regions $\pi F \ll \exp(-s_{\perp}^{\max})$, $\exp(-s_{\perp}^{\max}) \ll \pi F \ll 1$, $1 \ll \pi F \ll \exp(s_{\parallel}^{\max})/2$, and $\exp(s_{\parallel}^{\max})/2 \ll \pi F$. If the conditions in Eqs. (12) and (13) are not fulfilled then the two intermediate frequency intervals will disappear. Thus, it is the situation, the most interesting from the point of view of generality of the theoretical analysis, which is chosen in the following. It should be also mentioned that there are experimental indications³² that the attempt frequency itself might be significantly lower than the value $\propto 10^8$ – 10^{12} Hz presented above if there are mechanical resonances in the system that are able to enhance the role of low frequency phonons. In the microinhomogeneous systems these might be the resonances of the grains, perhaps.

To investigate both linear and nonlinear acoustic properties of the Preisach-Arrhenius model Eq. (8) is integrated. The exact solution subjected to the conditions of periodicity [$Q(\theta+1) = Q(\theta)$] is

$$Q = - \frac{\int_{\theta}^{\theta+1} d\theta' g_s(\theta') \exp\left[-\int_{\theta'}^{\theta+1} g_c(\theta'') d\theta''\right]}{1 - \exp\left[-\int_{\theta}^{\theta+1} g_c(\theta'') d\theta''\right]}, \quad (14)$$

where $g_s = (2/F)\exp(-s_{\perp})\sinh(s(\theta) - s_{\parallel})$, $g_c = (2/F)\exp(-s_{\perp}) \times \cosh(s(\theta) - s_{\parallel})$. It can be verified that if the distribution $\Delta\sigma'f$ has the symmetry property $\Delta\sigma'(s_{\parallel})f(s_{\parallel}) = \Delta\sigma'(-s_{\parallel}) \times f(-s_{\parallel})$ [which reduces to $s_{\parallel}^{\max} = |s_{\parallel}^{\min}|$ in the model (10)], then in addition to periodicity $\sigma(\theta+1) = \sigma(\theta)$ the stress satisfies the condition $\sigma(\theta+1/2) = -\sigma(\theta)$. The latter equality ensures that the nonlinearity of the system is of the odd type. Even type nonlinearity can exist in the PA model only due to the asymmetry of the $\Delta\sigma'f$ distribution relative to $\sqrt{2}s_{\perp}$ axis of the PM plane. It is worth mentioning here that even type nonlinearities do not shift the resonance frequencies of the bars.

In Fig. 4 the results of the numerical evaluation of the hysteresis stress/strain loops predicted by Eqs. (10) and (14) are presented for the particular case of sinusoidal strain variation and homogeneous element distribution inside the

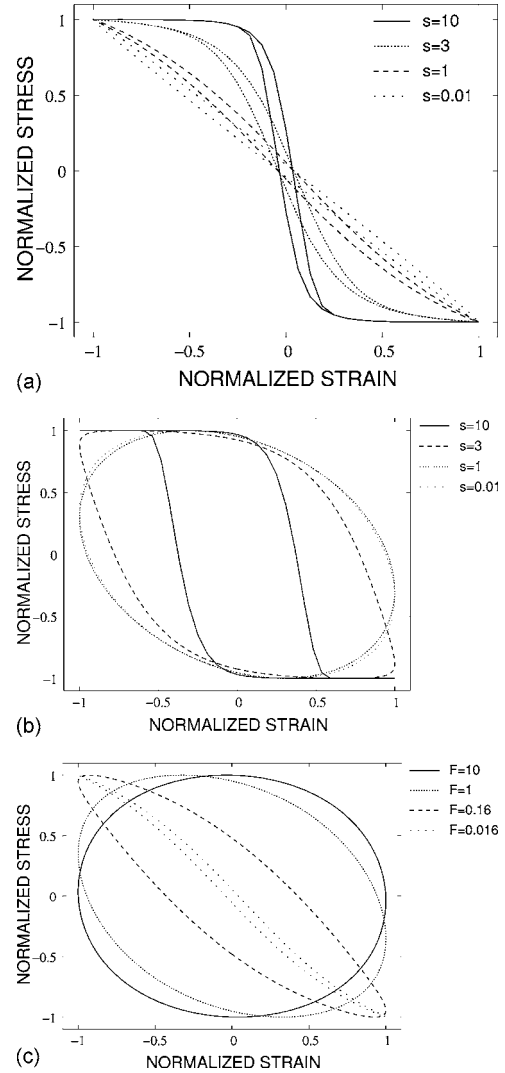


FIG. 4. Numerically obtained normalized stress/strain hysteretic dependences in the case of homogeneous element distribution inside the rectangular $s_{\perp} \leq 10$, $-10 \leq s_{\parallel} \leq 10$. The path of the system state variation is directed clockwise along the loops. Modification of the hysteresis loop with increasing wave amplitude at fixed frequency $F=0.016$ (a). Modification of the hysteresis loop with increasing wave amplitude at fixed frequency $F=1$ (b). Modification of the hysteresis loop with increasing frequency for the fixed wave amplitude $s_A=1$ (c).

rectangular $s_{\perp} \leq s_{\perp}^{\max} = 10$, $-10 = s_{\parallel}^{\min} \leq s_{\parallel} \leq s_{\parallel}^{\max} = 10$. The path of the system state variation is directed clockwise along the loops. Modification of the hysteresis loop with increasing wave amplitude at fixed low nondimensional frequency $F = 0.016$ is demonstrated in Fig. 4(a). Modification of the hysteresis loop with increasing wave amplitude at intermediate nondimensional frequency $F = 1$ is demonstrated in Fig. 4(b). Modification of the hysteresis loop with increasing frequency for the fixed wave amplitude $s_A = 1$ is demonstrated in Fig. 4(c). The transformation of an elliptical loop (typical for linear hysteresis in stress/strain relationship) to a nonelliptical loop (typical of nonlinear hysteresis) with increasing wave amplitude is clearly seen in Figs. 4(a) and 4(b). Comparison of the loops presented in Figs. 4(a) and 4(b) for the same

amplitude of strain, as well as Fig. 4(c) demonstrate the opening of hysteresis loops with increasing frequency, indicating a dynamic nature of hysteresis phenomenon captured by the Preisach-Arrhenius model.

The solution for the stress provided by Eqs. (10) and (14) will be used later for the evaluation of the system response in the case of the high amplitude acoustic loading (when the inequality $s_A \gg 1$ is valid for the acoustic wave amplitude normalized to s_0). For the analytical evaluation of the PA model behavior in some other limiting cases it appeared to be more suitable and much more instructive to find solutions for the asymptotic approximations of Eq. (8) than to fulfill asymptotic expansions of the exact solution (14).

III. QUASIEQUILIBRIUM STRESS/STRAIN RELATIONSHIPS

For the analysis of the quasiequilibrium (low frequency, quasistationary, quasistatic) response of the Preisach-Arrhenius system of hysteretic mechanical elements to acoustic loading it is useful to rewrite Eq. (8) as

$$Q = -\tanh(s - s_{\parallel}) + \left(-\frac{F \exp(s_{\perp})}{2 \cosh(s - s_{\parallel})} \right) \frac{\partial Q}{\partial \theta}. \quad (15)$$

The quasistationary solution (7) of Eq. (15) $Q_0 = -\tanh(s - s_{\parallel})$ is obtained by neglecting the derivative over time in the right-hand side (r.h.s.) of Eq. (15). The corrections to this solution are obtained by successive approximations, resulting in the following exact analytical solution:

$$Q = \sum_{n=0}^{\infty} Q_n = -\sum_{n=0}^{\infty} \left(-\frac{F \exp(s_{\perp})}{2 \cosh(s - s_{\parallel})} \right)^n \frac{\partial^n}{\partial \theta^n} \tanh(s - s_{\parallel}). \quad (16)$$

Surely solution (16) is valuable only if it is possible to use the limited (finite) number of terms in it. In other words the series (16) should contain a small parameter giving opportunity to neglect the higher order terms in the analysis. The leading terms of the expansion (16) are

$$\begin{aligned} Q_0 &= -\tanh(s - s_{\parallel}), & Q_1 &= \left(\frac{F \exp(s_{\perp})}{2} \right) \frac{1}{\cosh^3(s - s_{\parallel})} \frac{\partial s}{\partial \theta}, \\ Q_2 &= -\left(\frac{F \exp(s_{\perp})}{2} \right)^2 \frac{1}{\cosh^4(s - s_{\parallel})} \left[\frac{\partial^2 s}{\partial \theta^2} - 2 \tanh(s - s_{\parallel}) \right. \\ &\quad \left. \times \left(\frac{\partial s}{\partial \theta} \right)^2 \right]. \end{aligned} \quad (17)$$

It is straightforward to formulate sufficient conditions when the successive terms Q_n in Eq. (17) are smaller and smaller in amplitude for all the elements in the PM plane. It is sufficient to require $\pi F \ll \exp(-s_{\perp}^{\max})$. To derive this inequality it has been taken into account that (for the acoustic loading s expressed in terms of trigonometric functions) each differentiation over time θ provides additional multiplier 2π . When using Eq. (16) or Eq. (17), all the integrations in Eq. (10) can be done analytically for all n . The leading terms of the series $\sigma = \sum_{n=0}^{\infty} \sigma_n$ are

$$\begin{aligned} \sigma_0 &= s_{\perp}^{\max} [\ln(\cosh y)]_{y=-|s_{\parallel}^{\min}|}^{y=s_{\parallel}^{\max}-s}, \\ \sigma_1 &= \left(\frac{F \exp(s_{\perp}^{\max})}{2} \right) \frac{1}{2} \left[\frac{\tanh(y)}{\cosh(y)} \right. \\ &\quad \left. - \arctan(\sinh y) \right]_{y=-|s_{\parallel}^{\min}|}^{y=s_{\parallel}^{\max}-s} \left(\frac{\partial s}{\partial \theta} \right), \\ \sigma_2 &= -\frac{1}{2} \left(\frac{F \exp(s_{\perp}^{\max})}{2} \right)^2 \left\{ \left[\tanh(y) - \frac{\tanh^3(y)}{3} \right]_{y=-|s_{\parallel}^{\min}|}^{y=s_{\parallel}^{\max}-s} \right. \\ &\quad \left. \times \left(\frac{\partial^2 s}{\partial \theta^2} \right) + \left[\frac{1}{2 \cosh^4(y)} \right]_{y=-|s_{\parallel}^{\min}|}^{y=s_{\parallel}^{\max}-s} \left(\frac{\partial s}{\partial \theta} \right)^2 \right\}. \end{aligned} \quad (18)$$

Here and everywhere in the following the stress is normalized to the characteristic value $(\Delta \sigma' f)_0 s_0^2$ and the inequalities (12) and (13) are used to simplify the formulas where it is possible.

First the low-amplitude asymptotic behavior of the solution (18) is analyzed under the condition $s_A \ll s_{\parallel}^{\max}$, $|s_{\parallel}^{\min}|$. In the following as before we will always consider that $s_{\parallel}^{\max} \ll |s_{\parallel}^{\min}|$ and will never analyze the intermediate situations $s_{\parallel}^{\max} \ll s \ll |s_{\parallel}^{\min}|$ or $s_{\parallel}^{\max} \gg s \gg |s_{\parallel}^{\min}|$. Retaining in the Taylor expansion of Eq. (18) only the terms up to the third order in excitation amplitude, it is derived

$$\begin{aligned} \sigma_0 &\approx s_{\perp}^{\max} \left\{ s_{\parallel}^{\max} - |s_{\parallel}^{\min}| - 2s + 2[e^{-2s_{\parallel}^{\max}} - e^{-2|s_{\parallel}^{\min}|}]s^2 \right. \\ &\quad \left. + \frac{4}{3}[e^{-2s_{\parallel}^{\max}} + e^{-2|s_{\parallel}^{\min}|}]s^3 \right\}, \\ \sigma_1 &\approx \left(\frac{F}{2} e^{s_{\perp}^{\max}} \right) \left\{ \frac{\pi}{2} \frac{\partial s}{\partial \theta} - 8[e^{-3s_{\parallel}^{\max}} - e^{-3|s_{\parallel}^{\min}|}]s \frac{\partial s}{\partial \theta} \right. \\ &\quad \left. - 12[e^{-3s_{\parallel}^{\max}} + e^{-3|s_{\parallel}^{\min}|}]s^2 \frac{\partial s}{\partial \theta} \right\}, \\ \sigma_2 &\approx -\frac{1}{2} \left(\frac{F}{2} e^{s_{\perp}^{\max}} \right)^2 \left\{ \frac{4}{3} \frac{\partial^2 s}{\partial \theta^2} - 16[e^{-4s_{\parallel}^{\max}} - e^{-4|s_{\parallel}^{\min}|}] \left[s \frac{\partial^2 s}{\partial \theta^2} \right. \right. \\ &\quad \left. \left. - \frac{1}{2} \left(\frac{\partial s}{\partial \theta} \right)^2 \right] - 32[e^{-4s_{\parallel}^{\max}} + e^{-4|s_{\parallel}^{\min}|}] \left[s^2 \frac{\partial^2 s}{\partial \theta^2} - s \left(\frac{\partial s}{\partial \theta} \right)^2 \right] \right\}. \end{aligned} \quad (19)$$

The structure of the derived asymptotic solution (19) demonstrates that it is a valuable expansion at low frequencies in terms of the small parameter $\pi F \exp(s_{\perp}^{\max}) \ll 1$, because the terms of the same order in wave amplitude contributing to different σ_n are decreasing with increasing integer n under the latter condition. Consequently the derived solution provides asymptotic description of the quasiequilibrium regime defined by the inequality $\pi F \ll \exp(-s_{\perp}^{\max})$.

For the description of the dispersion of the particular nonlinear effects only the leading order term in the parameter $\pi F \exp(s_{\perp}^{\max}) \ll 1$ should be retained. The analysis of Eq. (19) leads to the following conclusions.

(1) In the case of the asymmetric distribution of the elements ($s_{\parallel}^{\max} \neq |s_{\parallel}^{\min}|$) there is a residual stress (strain indepen-

dent contribution to σ_0), which does not influence the propagation of the acoustic waves.

(2) The stress component $\sigma^{(1)}$ (describing the linear properties of the material) can be approximated as

$$\sigma^{(1)} \approx -2s_{\perp}^{\max}s + \left(\frac{F \exp(s_{\perp}^{\max})}{2} \right) \frac{\pi}{2} \frac{\partial s}{\partial \theta}. \quad (20)$$

Due to the condition $\pi F \exp(s_{\perp}^{\max}) \ll 1$ the second term in Eq. (20) is significantly smaller than the first one. However it should be retained to describe hysteretic linear absorption of the acoustic waves. In fact, the decrement of the acoustic wave D is proportional to the work done by the wave in a period $[D = \int_{\theta}^{\theta+1} \sigma ds / (2W) = \int_{\theta}^{\theta+1} \sigma (\partial s / \partial \theta) d\theta / (2W)]$, where $W \propto s_A^2$ is the energy density in the wave averaged over acoustic period]. In the case of the sinusoidal loading $W \approx E_0 s_A^2 / 2$, where E_0 denotes the elastic modulus of material in the absence of small contribution from the hysteretic elements. In accordance with this relation only the second term of Eq. (20) (which is out-of-phase with strain variation) contributes to linear absorption of sound. To get positive losses and stability of the system in response to weak acoustic perturbations it should be admitted that $\Delta\sigma'$ is positive as it has been explicitly assumed in Fig. 1. Consequently, in the following it should not be forgotten that the stress is normalized to the positive value $(\Delta\sigma' f)_0 s_0^2 > 0$. The linear decrement in the Preisach-Arrhenius model in the quasiequilibrium conditions is proportional to acoustic frequency ($D^{(1)} \propto F s_A^0$). This corresponds to linear absorption coefficient $\alpha^{(1)}$ proportional to square of frequency ($\alpha^{(1)} \propto D^{(1)} F \propto F^2 s_A^0$). The first term in Eq. (20) describes the linear contribution $E^{(1)}$ of the hysteretic elements to elastic modulus. For the analysis presented in the following it is sufficient to use for the evaluation of the hysteretic elements contribution E to the elastic modulus the relation $E = \int_{\theta}^{\theta+1} (\partial \sigma / \partial s) d\theta$. In the quasiequilibrium regime $E^{(1)}$ is found to be frequency-independent in the leading order ($E^{(1)} \propto -F^0 s_A^0$). Note that the presence of hysteretic elements causes the softening of the material due to $\Delta\sigma' > 0$.

(3) The leading contribution to quadratic nonlinearity, responsible for the second harmonic excitation and rectification process, also appears to be frequency-independent in the leading order,

$$\sigma^{(2)} \approx 2s_{\perp}^{\max} [e^{-2s_{\parallel}^{\max}} - e^{-2|s_{\parallel}^{\min}|}] s^2. \quad (21)$$

The frequency-dependent corrections to $\sigma^{(2)}$ in Eq. (21) can be identified in Eq. (19), but they are weak in the considered approximation. In accordance with Eq. (21) what happens with the material due to rectification of the acoustic wave (i.e., expansion or contraction) depends on the sign of the difference $s_{\parallel}^{\max} - |s_{\parallel}^{\min}|$.

(4) The leading terms describing the cubic nonlinearity are

$$\begin{aligned} \sigma^{(3)} \approx & \frac{4}{3} s_{\perp}^{\max} [e^{-2s_{\parallel}^{\max}} + e^{-2|s_{\parallel}^{\min}|}] s^3 - 12 \left(\frac{F}{2} e^{s_{\perp}^{\max}} \right) [e^{-3s_{\parallel}^{\max}} \\ & + e^{-3|s_{\parallel}^{\min}|}] s^2 \frac{\partial s}{\partial \theta}. \end{aligned} \quad (22)$$

In accordance with Eq. (20) and Eq. (22) cubic nonlinearity in the quasiequilibrium regime of the PA model diminishes amplitude-independent contributions both to hysteretic absorption and to elastic modulus (i.e., the nonlinear contributions are of the opposite sign to linear contributions). In particular, cubic nonlinearity leads to transparency ($D^{(3)} \propto -F s_A^2$). It is worth noting here that the predicted frequency-dependent transparency for the PA model differs from the frequency-independent quasi-static induced absorption in the PM model also in its dependence on the wave amplitude. In the PM model the induced decrement is linear in wave amplitude for low-amplitude acoustic waves,^{1-4,14,15} while $D^{(3)}$ is proportional to the square of the wave amplitude. In accordance with Eq. (22) the nonlinear variation in the elastic modulus is frequency-independent in the leading approximation ($E^{(3)} \propto F^0 s_A^2$). It also differs in the dependence on the amplitude from what is expected in the PM model, where the variation of modulus is proportional to the wave amplitude.^{1-4,14,15} Note that in the quasiequilibrium PA model the material with increasing wave amplitude becomes stiffer while in the PM model it becomes softer.^{1-4,14,15} As it will be demonstrated later (in Secs. VI and VII) these differences are due to the fact that Preisach-Mayergoyts model does not correspond to the quasiequilibrium limit of the Preisach-Arrhenius model. From the physics point of view the quasiequilibrium limit of the PA model is also a quasi-nonhysteretic limit, where the behavior of the individual elements is much closer to one presented in Fig. 3 than to one presented in Fig. 1.

For the analysis of the high-amplitude asymptotic behavior of the solution (18) under the condition $s_A \gg s_{\parallel}^{\max}, |s_{\parallel}^{\min}|$ only the terms of the first order in s_{\parallel}^{\max} and $|s_{\parallel}^{\min}|$ are retained in the corresponding Taylor expansion

$$\begin{aligned} \sigma \approx & - (s_{\parallel}^{\max} + |s_{\parallel}^{\min}|) \left\{ s_{\perp}^{\max} \tanh(s) + \left(-\frac{F \exp(s_{\perp}^{\max})}{2} \right) \right. \\ & \times \frac{1}{\cosh^3(s)} \frac{\partial s}{\partial \theta} + \frac{1}{2} \left(-\frac{F \exp(s_{\perp}^{\max})}{2} \right)^2 \\ & \left. \times \left[\frac{1}{\cosh^4(s)} \frac{\partial^2 s}{\partial \theta^2} + 2 \frac{\tanh(s)}{\cosh^4(s)} \left(\frac{\partial s}{\partial \theta} \right)^2 \right] \right\}. \end{aligned} \quad (23)$$

Under the quasiequilibrium condition $\pi F \exp(s_{\perp}^{\max}) \ll 1$, Eq. (23) appears to be a nicely ordered expansion in this small parameter. In accordance with Eq. (23) the elastic modulus weakly depends on frequency. The leading frequency-independent contribution to stress describes stress saturation with increasing level of the acoustic excitation

$$\sigma^{\text{elastic}} \approx - (s_{\parallel}^{\max} + |s_{\parallel}^{\min}|) s_{\perp}^{\max} \tanh(s). \quad (24)$$

The structure of Eq. (24) [where σ^{elastic} is proportional to the total number of the hysteretic elements $\propto (s_{\parallel}^{\max} + |s_{\parallel}^{\min}|) s_{\perp}^{\max}$] indicates that the saturation is due to the fact that increasing

wave amplitude does not involve additional elements in the relaxation process. It should be noted that under the assumption $\exp(s_{\parallel}^{\max}) \gg 1$, assumed everywhere in the analysis, the condition $s_A \gg s_{\parallel}^{\max}, |s_{\parallel}^{\min}|$ requires $s_A \gg 1$. Using this condition it is possible to estimate the hysteretic modulus for the case of sinusoidal loading ($s = s_A \sin 2\pi\theta$) in the considered regime. It is found that $E \propto -Fs_A^{-1}$. The material becomes more and more rigid with increasing wave amplitude (we remind here that at very low amplitudes $E < 0$).

In order to get terms describing even elastic nonlinearity it is necessary to keep in expansion (23) also the terms proportional to $[(s_{\parallel}^{\max})^2 - (s_{\parallel}^{\min})^2]$ originating from the asymmetry of the element distribution. In the considered approximation they are at least by a factor of $[(s_{\parallel}^{\max}) - |s_{\parallel}^{\min}|]/s_A \ll 1$ smaller.

The leading inelastic contribution to stress $\sigma^{\text{inelastic}}$ in Eq. (23) is

$$\sigma^{\text{inelastic}} \approx (s_{\parallel}^{\max} + |s_{\parallel}^{\min}|) \left(\frac{F \exp(s_{\perp}^{\max})}{2} \right) \frac{1}{\cosh^3(s)} \frac{\partial s}{\partial \theta}. \quad (25)$$

It describes hysteretic absorption. Here and in the following we are using term inelastic for the stress component responsible for the irreversible losses of the acoustic energy. Using the condition $s_A \gg 1$, it is possible to estimate the hysteretic losses for the case of sinusoidal loading ($s = s_A \sin 2\pi\theta$) in the considered regime. It is found that $D \propto Fs_A^{-1}$. The material becomes more and more transparent with increasing wave amplitude. This prediction correlates with results obtained in Ref. 31 from the analysis of the Preisach-Mayergoyz model with element density decreasing in the normal direction to the PM plane diagonal.

The analysis of the limiting cases of low and high amplitude acoustic action demonstrated that increase of wave amplitude leads to induced transparency in the quasiequilibrium regime of the Preisach-Arrhenius system response. Detailed analysis of the $\sigma^{(1)}$ contribution in Eq. (18) indicates that this is true for arbitrary wave amplitudes.

IV. QUASIFROZEN STRESS/STRAIN RELATIONSHIP

The structure of Eq. (8) indicates that at high frequencies there might be possible to construct an asymptotic solution in the form of infinite series based on a small parameter proportional to $1/F \ll 1$. Taking into account, that the high frequency action on the system might be rectified (due to the nonlinearity of the process), the solution should be presented in the form $Q = \langle Q \rangle + \sum_{n=1}^{\infty} \tilde{Q}_n$, where $\langle Q \rangle$ is the time-independent (averaged over the wave period) contribution, while the subsequent terms are expected to be of increasing order of smallness in terms of a parameter proportional to $1/F \ll 1$. Note that $\langle \tilde{Q}_n \rangle = 0$. By substitution of this series in Eq. (8) and averaging, the solution for $\langle Q \rangle$ is obtained in the form

$$\langle Q \rangle = - \frac{1}{\langle \cosh(s - s_{\parallel}) \rangle} \left[\langle \sinh(s - s_{\parallel}) \rangle - \sum_{n=1}^{\infty} \langle \cosh(s - s_{\parallel}) \tilde{Q}_n \rangle \right].$$

Then, by grouping the terms of the same order, it is possible to construct the following formally precise solution for the derivative $\partial Q / \partial \theta = \sum_{n=1}^{\infty} \partial \tilde{Q}_n / \partial \theta$

$$\begin{aligned} \frac{\partial \tilde{Q}_1}{\partial \theta} &= - \frac{2}{F} e^{-s_{\perp}} \cosh(s - s_{\parallel}) \left[\tanh(s - s_{\parallel}) - \frac{\langle \sinh(s - s_{\parallel}) \rangle}{\langle \cosh(s - s_{\parallel}) \rangle} \right], \\ \frac{\partial \tilde{Q}_{n \geq 2}}{\partial \theta} &= \frac{2}{F} e^{-s_{\perp}} \cosh(s - s_{\parallel}) \left[\tilde{Q}_{n-1} - \frac{\langle \cosh(s - s_{\parallel}) \tilde{Q}_{n-1} \rangle}{\langle \cosh(s - s_{\parallel}) \rangle} \right]. \end{aligned} \quad (26)$$

For the calculation of averages it should be taken into account that, for the periodic process s symmetrical relative to $s=0$ and, consequently, with zero average $\langle s \rangle = 0$, the equality $\langle \sinh s \rangle = 0$ holds. This provides opportunity to evaluate the leading frequency-dependent oscillating contribution to Q rate in Eq. (26),

$$\frac{\partial \tilde{Q}_1}{\partial \theta} = - \frac{2}{F} e^{-s_{\perp}} \frac{1}{\cosh(s_{\parallel})} \sinh s. \quad (27)$$

When Eq. (27) is substituted into Eq. (10) it gives opportunity to find the leading contribution to stress rate

$$\frac{\partial \tilde{\sigma}_1}{\partial \theta} \approx - \frac{2\pi}{F} \sinh s. \quad (28)$$

Comparison of Eq. (28) with the next term $\partial \tilde{\sigma}_2 / \partial \theta$ of the stress rate expansion evaluated with the help of $\partial \tilde{Q}_2 / \partial \theta$ indicates that the solution (28) provides the leading contribution to strain rate under the condition

$$(1/\pi F) s_{\parallel}^{\max} \exp(|s|) \ll 1. \quad (29)$$

Note that in the simplification of Eq. (29) the assumption $s_{\parallel}^{\max} \propto |s_{\parallel}^{\min}|$ has been extensively used. For the fixed high frequency $\pi F \gg 1$, Eq. (29) provides the restrictions on wave amplitude necessary for the validity of Eq. (28). From a physics point of view the validity of the quasifrozen asymptotic is always possible only in some restricted domain of wave amplitudes, because the relaxation frequency of the elements increases with wave amplitude. In fact, it is the coefficient $\omega = (2/\tau_0) \exp(-s_{\perp}) \cosh(s - s_{\parallel})$ in front of the second term in Eq. (8) that plays the role of the relaxation frequency in the presence of the acoustic loading. Its averaging over the wave period provides the qualitative description of the average relaxation frequency

$$\langle \omega \rangle = (2/\tau_0) \exp(-s_{\perp}) \cosh(s_{\parallel}) \langle \cosh(s) \rangle. \quad (30)$$

The relation (30) indicates the increase in the relaxation frequency of all the elements with increasing level of the acoustic excitation. Consequently, if the wave amplitude can increase without restriction, then sooner or later for the fixed excitation frequency the elements will be transformed from quasifrozen to quasiequilibrium.

The solution (28) provides opportunity to evaluate the leading contribution to hysteretic decrement $[D = \int_{\theta}^{\theta+1} \sigma ds / (2W) = -\int_{\theta}^{\theta+1} s d\sigma / (2W) = -\int_{\theta}^{\theta+1} s(\partial\sigma/\partial\theta) d\theta / (2W)]$ at high frequencies of the acoustic action. Calculations for the case of the sinusoidal loading lead to the conclusion that in the quasifrozen regime the increase in wave amplitude induces absorption. In the low-amplitude limit ($s_A \ll 1$) the dependence of the decrement on frequency and amplitude is $D \propto F^{-1}[1 + (3/4)s_A^2 + \dots]$. In the high-amplitude limit ($s_A \gg 1$) it is found that $D \propto F^{-1}s_A^{-3/2} \exp(s_A)$. It is worth reminding that the latter high-amplitude asymptotic is valid in the restricted range of wave amplitudes. Though with increasing F the obtained solution is valid for higher and higher wave amplitudes [in the region $s_A \leq \ln(\pi F/s_{\parallel}^{\max})$] the acoustic decrement at this upper boundary diminishes ($D \propto s_A^{-3/2}$) when the boundary becomes higher.

Importantly, from the derived asymptotic expansions it follows that the magnitude of the contribution of hysteretic elements to elastic modulus diminishes at very high frequencies (corresponding to the quasifrozen regime) faster than proportionally to $1/F$. This prediction will be confirmed by the low-amplitude asymptotic solution derived in the next section.

V. STRESS/STRAIN RELATIONSHIP FOR LOW-AMPLITUDE ACOUSTIC LOADING

To solve Eq. (8) in the case of weak acoustic loading we are substituting in it formal Taylor expansions of the functions $\cosh(s-s_{\parallel})$ and $\sinh(s-s_{\parallel})$ for $|s| \ll |s_{\parallel}|$. Then Eq. (8) takes the form

$$\begin{aligned} \partial Q / \partial \theta + \gamma \left[\sum_{n=0}^{\infty} (-\beta)^{[1+(-1)^n]/2} s^n / n! \right] Q \\ = -\gamma \left[\sum_{n=0}^{\infty} (-\beta)^{[1+(-1)^n]/2} s^n / n! \right]. \end{aligned} \quad (31)$$

Here the notations $\gamma = (2/F) \exp(-s_{\perp}) \cosh(s_{\parallel}) \equiv \omega_0 T$ and $\beta = \tanh(s_{\parallel})$ are introduced. The solution in the form $Q = \sum_{n=0}^{\infty} Q_n$ (where Q_n is assumed to be of the order s^n) is substituted in Eq. (31) and the terms of the same order in powers of s are grouped into separate equations

$$\begin{aligned} \partial Q_n / \partial \theta + \gamma Q_n = -\gamma \left[(-\beta)^{[1+(-1)^n]/2} s^n / n! \right. \\ \left. + \sum_{m=1}^n (-\beta)^{[1+(-1)^m]/2} Q_{n-m} s^m / m! \right]. \end{aligned} \quad (32)$$

The obtained equations in Eq. (32) can be solved successively one after another, taking into account that $\partial Q_0 / \partial \theta = 0$ and that all Q_n should be periodic. The solutions for Q_1 and Q_2 found for the sinusoidal excitation $s = s_A \sin(2\pi\theta)$ are

$$Q_1 = -s_A (1 - \beta^2) \frac{\gamma^2}{\gamma^2 + (2\pi)^2} \left\{ \sin(2\pi\theta) - \frac{2\pi}{\gamma} \cos(2\pi\theta) \right\}, \quad (33)$$

$$\begin{aligned} Q_2 = -s_A^2 \frac{\beta(1 - \beta^2)}{2} \frac{\gamma^2}{\gamma^2 + (2\pi)^2} \\ \times \left\{ 1 - \operatorname{Re} \left[\frac{\gamma - i2\pi}{\gamma + i4\pi} \exp(i4\pi\theta) \right] \right\}. \end{aligned} \quad (34)$$

In the solution for Q_3 only the contributions at the fundamental frequency (responsible for nonlinear induced variations of elastic modulus and hysteretic absorption) are retained while the terms describing the third harmonic excitation are omitted for compactness

$$\begin{aligned} Q_3 = -s_A^3 \frac{(1 - \beta^2)}{4} \left\{ \left[(1 - \beta^2) \frac{\gamma^2}{\gamma^2 + (2\pi)^2} + 4\beta^2 \frac{\gamma^2}{\gamma^2 + (4\pi)^2} \right. \right. \\ \left. \left. - 2 \frac{\gamma^4}{[\gamma^2 + (2\pi)^2]^2} \right] \sin(2\pi\theta) - \pi \left[(1 - 4\beta^2) \frac{\gamma}{\gamma^2 + (2\pi)^2} \right. \right. \\ \left. \left. + 16\beta^2 \frac{\gamma}{\gamma^2 + (4\pi)^2} - 4 \frac{\gamma^3}{[\gamma^2 + (2\pi)^2]^2} \right] \cos(2\pi\theta) \right\}. \end{aligned} \quad (35)$$

The conditions for the validity of the obtained solution are derived by the comparison of the different contributions to the successive terms. From the comparison of the amplitudes $|Q_1|$ from Eq. (33) and $|Q_2|$ from Eq. (34) it follows that the condition $\beta s_A = \tanh(s_{\parallel}) s_A \ll \sqrt{1 + (2\pi/\gamma)^2}$ is required. In general the domain of validity of the obtained results depends on the excitation frequency and the wave amplitude. In particular, the condition for the validity improves with increasing frequency. Under the assumed condition $\exp(s_{\parallel}^{\max}) \propto \exp(|s_{\parallel}^{\min}|) \gg 1$, the inequality $\beta s_A = \tanh(s_{\parallel}) s_A \ll \sqrt{1 + (2\pi/\gamma)^2}$ is satisfied in the whole part of the PM plane occupied by the hysteretic elements and at all frequencies if $s_A \ll 1$. So the latter inequality will be assumed in what follows in this section.

To obtain the linear stress/strain relationship, the solution for Q_1 [Eq. (33)] is substituted into the integral (10). Using γ and $x = \cosh(s_{\parallel})$ as new integration variables ($ds_{\perp} = -d\gamma/\gamma$, $ds_{\parallel} = dx/\sqrt{x^2 - 1}$) the result for the normalized stress after the integration over γ is presented in the form

$$\begin{aligned} \sigma_1 \approx s_A \int_{1,1}^{\exp(s_{\parallel}^{\max})/2, \exp(|s_{\parallel}^{\min}|)/2} \frac{dx}{x^2 \sqrt{x^2 - 1}} \left\{ \frac{1}{2} \ln(1 \right. \\ \left. + \gamma^2) \sin(2\pi\theta) - \arctan(\gamma) \cos(2\pi\theta) \right\} \begin{matrix} x e^{-s_{\perp}^{\max}} / (\pi F) \\ x / (\pi F) \end{matrix}. \end{aligned} \quad (36)$$

The linear acoustic decrement is proportional to the cosine component σ_1^c of σ_1 . Due to the assumption (12) the asymptotic behavior of σ_1^c can be evaluated in three large successive frequency ranges as

$$\sigma_1^c/s_A \approx \begin{cases} (\pi^2/2)\exp(-s_\perp^{\max})F \propto F, & \pi F \ll \exp(-s_\perp^{\max}); \\ \pi \propto F^0, & \exp(-s_\perp^{\max}) \ll \pi F \ll 1; \\ 1/F \propto F^{-1}, & 1 \ll \pi F. \end{cases} \quad (37)$$

In practice the extraction of the asymptotics in Eq. (37) from Eq. (36) is significantly simplified by the observation that the factor $1/(x^2\sqrt{x^2-1})$ cuts the integration in Eq. (36) above $x \approx 2-3$. The solution in Eq. (37) predicts the resonance curve of the linear hysteretic absorption with a broad absolutely flat extremum. The predicted dependence of the linear decrement $D^{(1)}$ on frequency is qualitatively presented in Fig. 5(a). The low-frequency ($\propto F$) and the high-frequency ($\propto F^{-1}$) behavior precisely coincides with the description obtained earlier in Secs. III and IV, respectively. Importantly, the Preisach-Arrhenius theory naturally predicts that linear acoustic decrement might be frequency-independent in the broad frequency range $\exp(-s_\perp^{\max}) \ll \pi F \ll 1$. This corresponds to absorption coefficient of acoustic wave linearly increasing with frequency. Consequently, thermally activated relaxation of hysteretic mechanical elements can provide contribution to this type of absorption ($\alpha^{(1)} \propto F$) observed in multiple experiments on different types of microinhomogeneous materials.³³⁻³⁶ It should be mentioned that currently there is

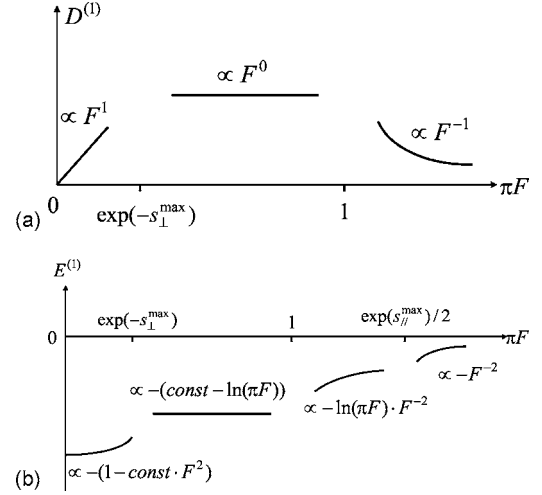


FIG. 5. Schematic illustration of the variation with frequency of the amplitude-independent decrement $D^{(1)}$ (a) and of the amplitude-independent modulus defect $E^{(1)}$ (b) in the case of the low-amplitude acoustic loading.

no consensus on the mechanism of this experimentally observed absorption.^{33,34,37-41}

The sine component σ_1^s of σ_1 describes contribution of hysteretic elements to elastic modulus. The asymptotic behavior of this component can be described by

$$\sigma_1^s/s_A \approx \begin{cases} -2s_\perp^{\max}\{1 - [\exp(2s_\perp^{\max})/3s_\perp^{\max}](\pi F)^2\}, & \pi F \ll \exp(-s_\perp^{\max}); \\ -2[1 - \ln 2 - \ln(\pi F)], & \ln(\sqrt{s_\perp^{\max}})\exp(-s_\perp^{\max}) \ll \pi F \ll 1; \\ -2 \ln(\pi F)/(\pi F)^2, & 1 \ll \pi F \ll \exp(s_\parallel^{\max})/2, \exp(|s_\parallel^{\min}|)/2; \\ -(1/2)(s_\parallel^{\max} + |s_\parallel^{\min}|)/(\pi F)^2 \propto F^{-2}, & \exp(s_\parallel^{\max})/2, \exp(|s_\parallel^{\min}|)/2 \ll \pi F. \end{cases} \quad (38)$$

Solution (38) describes that material becomes progressively more and more rigid with increasing frequency. The low frequency asymptotic in Eq. (38) coincides with one derived in Sec. III. The prediction that at high frequencies ($\pi F \gg 1$) the contribution to modulus falls faster than inverse proportionally to frequency also correlates with the analysis of the quasifrozen regime in Sec. IV. The predicted dependence of the linear modulus $E^{(1)}$ variation on frequency is qualitatively presented in Fig. 5(b). It should be mentioned that due to the factor $1/(x^2\sqrt{x^2-1})$ in Eq. (36) the integration limits over s_\parallel play role only in the evaluation of the last of the asymptotics from those presented in Eqs. (37) and (38). It is also worth mentioning that most of the boundaries between the different frequency regions in Eq. (37), Eq. (38) and in the analysis presented later in this section coincide with the characteristic frequencies defined in Sec. II on the basis of qualitative arguments.

The structure of Q_2 in Eq. (34), where the multiplier $\beta = \tanh(s_\parallel)$ makes it an odd function of s_\parallel , suppresses its contribution to stress by reducing the integration space over s_\parallel to

the interval between s_\parallel^{\max} and $|s_\parallel^{\min}|$ (in comparison with the integration region $-|s_\parallel^{\min}| \leq s \leq s_\parallel^{\max}$ effective for Q_1 and Q_3). Here only the dispersion of the demodulation (rectification) process caused by the quadratic nonlinearity will be demonstrated. The dependence on frequency of the processes responsible for the second harmonic excitation [second term in Eq. (34)] is expected to be qualitatively similar. Evaluating with the help of the first term in Eq. (34) the time-independent contribution σ_2^0 to stress, it is obtained

$$\sigma_2^0 \approx s_A^2 \int_{\exp(|s_\parallel^{\min}|)/2}^{\exp(s_\parallel^{\max})/2} \frac{dx}{x^3} \left\{ \frac{1}{2} \ln(1 + \gamma^2) \right\}_{x^j(\pi F)}^{x \exp(-s_\perp^{\max})/(\pi F)}. \quad (39)$$

Solution (39) demonstrates once again that quadratic nonlinearity in the system can be due only to the asymmetry of the element distribution. The asymptotic behavior of the quadratic nonlinearity in different frequency intervals is described by

$$\sigma_2^0/s_A^2 \approx \begin{cases} -2s_{\perp}^{\max}[e^{-2|s_{\parallel}^{\min}|} - e^{-2s_{\parallel}^{\max}}][1 - (e^{2s_{\perp}^{\max}}/s_{\perp}^{\max})[e^{-2|s_{\parallel}^{\min}|} + e^{-2s_{\parallel}^{\max}}](\pi F)^2], & \pi F \ll e^{(s_{\parallel}^{\max}-s_{\perp}^{\max})/2}; \\ -\frac{1}{2}[(|s_{\parallel}^{\min}|e^{-2|s_{\parallel}^{\min}|} - s_{\parallel}^{\max}e^{-2s_{\parallel}^{\max}} - (e^{-2|s_{\parallel}^{\min}|} - e^{-2s_{\parallel}^{\max}})\ln(\pi F)], & e^{(s_{\parallel}^{\max}-s_{\perp}^{\max})/2} \ll \pi F \ll e^{s_{\parallel}^{\max}/2}; \\ -(1/2)(s_{\parallel}^{\max} - |s_{\parallel}^{\min}|)/(\pi F)^2 \propto F^{-2}, & e^{s_{\parallel}^{\max}}/2 \ll \pi F. \end{cases}$$

Here Eq. (13) has been applied in order to reduce the number of different possible regimes. According to the derived formulas the dispersion of quadratic nonlinearity is very weak except for very high frequencies. The sign of the stress providing rectification always depends on the relative magnitude

of s_{\parallel}^{\max} and $|s_{\parallel}^{\min}|$ as it has been already noticed for the quasiequilibrium regime in Sec. III.

For the evaluation of the cubic nonlinearity, influencing the propagation of the wave at fundamental frequency, the solution (35) is substituted in Eq. (10) and integrated over γ

$$\sigma_3 \approx s_A^3 \frac{1}{8} \int_{1,1}^{\exp(s_{\parallel}^{\max})/2, \exp(|s_{\parallel}^{\min}|)/2} \frac{dx}{x^2 \sqrt{x^2 - 1}} \left\{ \left(\frac{1}{x^2} - 2 \right) \ln \left[1 + \left(\frac{\gamma}{2\pi} \right)^2 \right] + 4 \left(1 - \frac{1}{x^2} \right) \ln \left[1 + \left(\frac{\gamma}{4\pi} \right)^2 \right] - \frac{2(\gamma/2\pi)^2}{1 + (\gamma/2\pi)^2} \right\} \sin(2\pi\theta) - \left\{ \left(\frac{4}{x^2} - 5 \right) \arctan \left(\frac{\gamma}{2\pi} \right) + 8 \left(1 - \frac{1}{x^2} \right) \arctan \left(\frac{\gamma}{4\pi} \right) + \frac{2(\gamma/2\pi)}{1 + (\gamma/2\pi)^2} \right\} \cos(2\pi\theta) \Bigg|_{x/(\pi F)}^{x \exp(-s_{\perp}^{\max})/(\pi F)}. \quad (40)$$

The behavior in the different frequency ranges of the cosine component σ_3^c in Eq. (40), responsible for the hysteretic absorption, is described by

$$\sigma_3^c/s_A^3 \approx \begin{cases} -(3/2)\{[e^{-3|s_{\parallel}^{\min}|} + e^{-3s_{\parallel}^{\max}}]\pi F e^{s_{\perp}^{\max}} + 32\pi(\pi F e^{s_{\perp}^{\max}})^3\}, & \pi F \ll e^{-s_{\perp}^{\max}}; \\ (\pi/24)\{1 - 3/(\pi F e^{s_{\perp}^{\max}})\} \propto F^0, & e^{-s_{\perp}^{\max}} \ll \pi F \ll 1; \\ (\pi/8)/(\pi F) \propto F^{-1}, & 1 \ll \pi F. \end{cases} \quad (41)$$

The predicted variation of the amplitude-dependent decrement $D^{(3)}$ with frequency is qualitatively presented in Fig. 6(a). At low frequencies [$\pi F \ll \exp(-s_{\perp}^{\max})$] the increase in wave amplitude induces transparency of the material. This prediction on the base of Eq. (41) correlates with one previously derived from quasiequilibrium asymptotic (Sec. III). However Eq. (41) provides additional new information on the low-frequency regime. It appears that the coefficient of the first term ($\propto -F$) due to the integration over the element distribution contains additional parameter of smallness [$\exp(-3s_{\parallel}^{\max}) \ll 1$] in comparison to the subsequent term. It can be concluded that $\sigma_3^c \propto -F$ only if $\pi F \gg [\exp(-3s_{\parallel}^{\max}/2)/4\sqrt{\pi}] \exp(-s_{\perp}^{\max}) \ll \exp(-s_{\perp}^{\max})$, while in the wide frequency region [$\exp(-3s_{\parallel}^{\max}/2)/4\sqrt{\pi}] \exp(-s_{\perp}^{\max}) \ll \pi F \ll \exp(-s_{\perp}^{\max})$] the induced transparency varies $\propto -F^3$. The prediction in Eq. (41) of the induced absorption in the high-frequency limit ($\pi F \gg 1$) correlates with the obtained

earlier asymptotic for the quasifrozen regime in Sec. IV. The theory predicts frequency-independence of the nonlinear decrement in the same frequency interval $\exp(-s_{\perp}^{\max}) \ll \pi F \ll 1$ as for the linear decrement [see Eq. (37)]. The transition from the induced transparency to the induced absorption takes place around $\pi F \propto \exp(-s_{\perp}^{\max})$.

It should be mentioned here that the low frequency [$\pi F \ll \exp(-s_{\perp}^{\max})$] asymptote in Eq. (41) provides an example when the descending character of the terms in the series $Q = \sum_{n=0}^{\infty} Q_n$ does not necessarily lead (after the integration over the PM plane) to the descending character of the terms in the series $\sigma = \sum_{n=0}^{\infty} \sigma_n$. The validity of the obtained leading asymptotic expansions for the stress should be always carefully examined from this point of view.

The dependence of the induced variations in the elastic modulus (and consequently in the wave velocity) is controlled by the sine component of Eq. (40)

$$\sigma_3^s/s_A^3 = \begin{cases} s_{\perp}^{\max} \{e^{-2s_{\parallel}^{\max}} + e^{-2|s_{\parallel}^{\min}|} + [2 \exp(2s_{\parallel}^{\max})/3s_{\parallel}^{\max}](\pi F)^2\}, & \pi F \ll \exp(-s_{\perp}^{\max}); \\ (1 + 2 \ln 2)/3, & \ln(\sqrt{s_{\parallel}^{\max}}) \exp(s_{\perp}^{\max}) \ll \pi F \ll 1; \\ (5/4) \ln(\pi F)/(\pi F)^2, & 1 \ll \pi F \ll \exp(s_{\parallel}^{\max})/2, \exp(|s_{\parallel}^{\min}|)/2; \\ (3/8)(s_{\parallel}^{\max} + |s_{\parallel}^{\min}|)/(\pi F)^2 \propto F_{-2} & \exp(s_{\parallel}^{\max})/2, \exp(|s_{\parallel}^{\min}|)/2 \ll \pi F \end{cases} \quad (42)$$

The predicted variation of the amplitude-dependent modulus $E^{(3)}$ with frequency is qualitatively presented in Fig. 6(b). The predictions in Eq. (42) correlate with the low and high frequency asymptotes from Secs. III and IV. Similar to the linear modulus, the nonlinear contribution to modulus weakly depends on frequency in the same intermediate frequency range as the acoustic decrement. However in comparison with the linear asymptotic in Eq. (38) the logarithmic behavior of the nonlinear modulus in this frequency interval cannot be guaranteed, because the logarithmic term appears to contain an additional small parameter [$\propto \exp(-3s_{\parallel}^{\max}) \ll 1$].

VI. DEFECT OF MODULUS FOR HIGH-AMPLITUDE ACOUSTIC LOADING

It should be clearly stated that none of the asymptotic regimes analyzed in the Secs. III–V has indicated the presence of the regime corresponding to Preisach-Mayergoyz model as a limiting case of the considered Preisach-Arrhenius model. The Preisach-Mayergoyz model predicts the decrement and modulus variation both proportional to acoustic wave amplitude s_A .^{4,14,15} Importantly, these amplitude-dependent contributions are the leading contributions, that is they exceed amplitude-independent contributions (which are completely absent in the Preisach-Mayergoyz model). An important condition for $D \propto s_A$ and $E \propto -s_A$ in the Preisach-Mayergoyz model is the assumption of the infinite extension of the homogeneous distribution of the elements in the PM plane (in other words $s_{\perp}^{\max} \rightarrow \infty$, $s_{\parallel}^{\max} \rightarrow \infty$, $s_{\parallel}^{\min} \rightarrow -\infty$). For example, in Ref. 31 the deviation from the linear dependences $D \propto s_A$ and $E \propto -s_A$ was predicted for the case when the element distribution cannot be considered homogeneous at the scale s_A of acoustic strain variation.

It follows, from what has been mentioned just above, that PM regime is definitely separated from the quasiequilibrium one, because for $s_{\perp}^{\max} \rightarrow \infty$ the conditions for the validity of the quasiequilibrium regime [$\pi F \ll \exp(-s_{\perp}^{\max})$] cannot be satisfied. PM regime is also separated from the quasifrozen regime, because for $s_{\parallel}^{\max} \propto |s_{\parallel}^{\min}| \rightarrow \infty$ the condition (29) ($\pi F \gg s_{\parallel}^{\max} \exp(|s_{\parallel}^{\min}|)$) for the validity of the latter regime cannot be satisfied. We conclude that PM regime should be located between the quasiequilibrium and the quasifrozen, as expected from physical considerations. At too low frequencies PM regime is absent because there is nearly no hysteresis (an element has enough time both in loading and unloading to take statistically the same equilibrium position). At too high frequencies the hysteresis is nearly absent because the ele-

ments have no time to switch from one level to another.

In Sec. V it was found that in the case of low amplitude acoustic loading, identified by the inequality $s_A \ll 1$, the leading contribution to the decrement and modulus are amplitude-independent. Consequently, the Preisach-Mayergoyz regime might be realized only if $s_A \gg 1$. Correspondingly, in this section the behavior of the Preisach-Arrhenius model under high amplitude loading ($s_A \gg 1$), which however is always in the region of the homogeneity of the elements distribution (formally $s_{\perp}^{\max} \rightarrow \infty$, $s_{\parallel}^{\max} \rightarrow \infty$, $s_{\parallel}^{\min} \rightarrow -\infty$), is analyzed. Even the asymptotic analysis is rather complicated in this regime. Below, a possible approach for the evaluation of the modulus defect is presented. The obtained results provide an opportunity to localize the PM regime inside the Preisach-Arrhenius model, that is to predict the conditions for its realization.

The modulus defect is defined here as an average over a wave period of the modulus variation induced by the bistable mechanical elements

$$\langle E \rangle = \frac{1}{2\pi} \oint \left(\frac{\partial \sigma}{\partial s} \right) d\theta, \quad (43)$$

where $\theta = \omega t$ is the nondimensional time variable. Sinusoidal strain variation in the acoustic wave will be approximated by a sawtooth profile of the form

$$s = \frac{2}{\pi} s_A \begin{cases} \theta, & -\pi/2 \leq \theta \leq \pi/2; \\ \pi - \theta, & \pi/2 \leq \theta \leq 3\pi/2. \end{cases} \quad (44)$$

Note, that in the wave (44) the fundamental frequency dominates (the third harmonic is at the level of 10% of the fundamental one). So this is a very reasonable approximation even for the quantitative estimates and not only for the qualitative evaluation. Importantly, in the wave (44) there is a very simple relation between the differentials ds and $d\theta$

$$d\theta = \frac{\pi}{2s_A} \begin{cases} ds, & -\pi/2 \leq \theta \leq \pi/2; \\ -ds, & \pi/2 \leq \theta \leq 3\pi/2. \end{cases} \quad (45)$$

With the help of Eq. (45) the integration in Eq. (43) is straightforward

$$\langle E \rangle = \frac{1}{2s_A} [\sigma(s = s_{\max} = s_A) - \sigma(s = s_{\min} = -s_A)]. \quad (46)$$

From Eq. (46) it follows that for the estimate of modulus defect $\langle E \rangle$ the knowledge of the details of the hysteretic loop is not necessary (it is sufficient to evaluate the stress values at maximum and minimum of strain). As it has been mentioned at the end of Sec. II for the elements distribution,

which is symmetric relative to the $\sqrt{2}s_{\perp}$ axis, the stress has odd symmetry [in particular, $\sigma(s=s_A)=-\sigma(s=-s_A)$] and Eq. (46) takes the form

$$\langle E \rangle = \frac{1}{s_A} \sigma(s=s_A). \quad (47)$$

The derived expression (47) for the modulus defect is known in literature as secant modulus.⁴² More precisely, the secant modulus is sometimes defined,⁴² as the ratio of modulus modification $\langle E \rangle$ in Eq. (47) and the linear modulus E_0 . In

accordance with Eq. (47) for the estimation of the secant modulus it is sufficient to estimate the stress at maximum of strain loading. Consequently, we need to evaluate Q in Eq. (14) at $\theta=\theta_{\max}$ corresponding to maximum of loading [$s(\theta=\theta_{\max})=s_{\max}=s_A$]. Surely, the latter is not necessarily equal to the maximum of the stress.

Due to the relations in Eq. (45) all the integrations over time can be replaced by the integrations over strain. Then the integrals in the powers of the exponentials are done precisely. The solution (14) for $Q(s=s_A)$ simplifies to the form

$$Q(s_A, s_{\parallel}) = -\alpha \left\{ \frac{e^{-\alpha[\sinh(s_A-s_{\parallel})+2\sinh(s_A+s_{\parallel})]}J(-\alpha, s_{\parallel}) + e^{-\alpha\sinh(s_A-s_{\parallel})}J(\alpha, s_{\parallel})}{1 - \exp(-4\alpha\sinh s_A \cosh s_{\parallel})} \right\}, \quad (48)$$

where

$$\alpha \equiv \frac{1}{4Fs_A} e^{-s_{\perp}},$$

and

$$J(\alpha, s_{\parallel}) \equiv \int_{-s_A}^{s_A} ds \sinh(s-s_{\parallel}) e^{\alpha\sinh(s-s_{\parallel})}.$$

The result in Eq. (48) should be substituted in Eq. (9) [or equivalently in Eq. (10)] for the integration over the PM plane. In the following, for the reasons discussed above, we will neglect inhomogeneity of the PM distribution of the elements in order to reveal the conditions where the so-called quadratic hysteretic nonlinearity [leading to $\sigma(s=s_A) \propto -s_A^2$ and, consequently, to $\langle E \rangle \propto -s_A$] might be realized. Due to the assumed symmetry of the distribution only the even in s_{\parallel} part of $Q(s_A, s_{\parallel})$ contributes to stress. Using the symmetry property $J(\alpha, -s_{\parallel}) = -J(-\alpha, s_{\parallel})$ of the function $J(\alpha, s_{\parallel})$ the part of Eq. (48), which is even in s_{\parallel} , is presented in the form

$$\begin{aligned} & \frac{Q(s_A, s_{\parallel}) + Q(s_A, -s_{\parallel})}{2} \\ &= \frac{\alpha}{2} \left\{ \frac{e^{-\alpha\sinh(s_A-s_{\parallel})}J(\alpha, s_{\parallel}) + e^{-\alpha\sinh(s_A+s_{\parallel})}J(\alpha, -s_{\parallel})}{1 + \exp(-2\alpha\sinh s_A \cosh s_{\parallel})} \right\}. \end{aligned} \quad (49)$$

Note an important point that in comparison with Eq. (48) the pole in the denominator of Eq. (49) has disappeared. The denominator in Eq. (49) is a function varying in a narrow limited interval (taking the values from 1 to 2). This variation has no influence on the asymptotic behavior of the stress and it will be omitted in what follows

$$\begin{aligned} \frac{Q(s_A, s_{\parallel}) + Q(s_A, -s_{\parallel})}{2} &\approx -\frac{\alpha}{2} \left[e^{-\alpha\sinh(s_A-s_{\parallel})}J(\alpha, s_{\parallel}) \right. \\ &\quad \left. + e^{-\alpha\sinh(s_A+s_{\parallel})}J(\alpha, -s_{\parallel}) \right]. \end{aligned} \quad (50)$$

In this approximation, when Eq. (50) is substituted in Eq. (10) (with $s_{\perp}^{\max} \rightarrow \infty$, $s_{\parallel}^{\max} \rightarrow \infty$, $s_{\parallel}^{\min} \rightarrow -\infty$), the integration over s_{\perp} is done precisely. This results in

$$\begin{aligned} \frac{\sigma(s=s_A)}{s_0^2(\Delta\sigma'f)_0} &\approx -\int_0^{\infty} ds_{\parallel} \int_{-s_A}^{s_A} ds \sinh(s-s_{\parallel}) \\ &\quad \times \left\{ \frac{e^{(1/2Fs_A)[\sinh(s-s_{\parallel})+\sinh(s_{\parallel}-s_A)]} - 1}{\sinh(s-s_{\parallel}) + \sinh(s_{\parallel}-s_A)} \right. \\ &\quad \left. - \frac{e^{(1/2Fs_A)[\sinh(s_{\parallel}-s)-\sinh(s_{\parallel}+s_A)]} - 1}{\sinh(s_{\parallel}-s) - \sinh(s_{\parallel}+s_A)} \right\}. \end{aligned} \quad (51)$$

Introducing the new variable z [$z=\sinh(s_{\parallel}-s)-\sinh(s_{\parallel}-s_A)$ and $z=\sinh(s-s_{\parallel})+\sinh(s_{\parallel}+s_A)$ in the first and in the second parts of the integral (51), respectively], we present Eq. (51) in the compact form

$$\begin{aligned} \bar{\sigma} &\equiv \frac{\sigma(s=s_A)}{s_0^2(\Delta\sigma'f)_0} \approx -\int_0^{\infty} ds_{\parallel} \int_0^{a+b} dz \left\{ \frac{1 - \exp[-z/(2Fs_A)]}{z} \right\} \\ &\quad \times \left\{ \frac{z-a}{\sqrt{1+(z-a)^2}} + \frac{z-b}{\sqrt{1+(z-b)^2}} \right\}, \end{aligned} \quad (52)$$

where $a(s_{\parallel}) \equiv \sinh(s_A+s_{\parallel})$, $b(s_{\parallel}) \equiv \sinh(s_A-s_{\parallel})$.

For the approximate integration of Eq. (52) we have used the following strategy (Fig. 7). First, the total integration region in the (s_{\parallel}, z) plane has been divided into two parts by the horizontal line $z=2Fs_A$. In the upper part, where $z \geq 2Fs_A$, the first function under the integral (52) is approximated by $1/z$. In the lower part $z \leq 2Fs_A$ it is approximated by

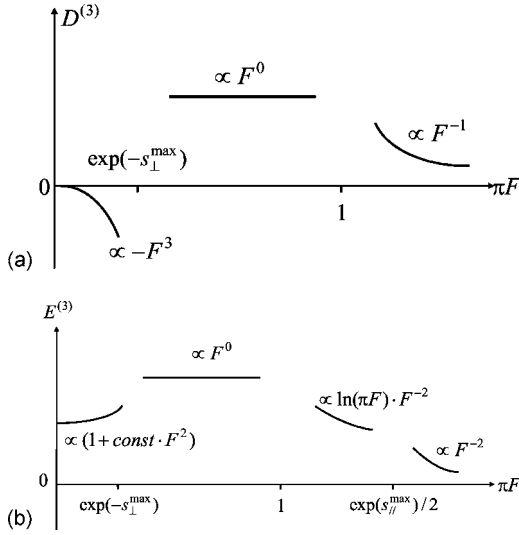


FIG. 6. Schematic illustration of the variation with frequency of the amplitude-dependent decrement $D^{(3)}$ (a) and of the amplitude-dependent modulus defect $E^{(3)}$ (b) in the case of the low-amplitude acoustic loading.

$$\frac{1}{2Fs_A} \left(1 - \frac{1}{4Fs_A} z \right).$$

Then the integration over z is straightforward. To integrate finally over s_{\parallel} the integration region is divided into separate areas by $s_{\parallel} = s_A$ and the vertical lines $s_{\parallel} = s_{a+b}$, $s_{\parallel} = s_a$, $s_{\parallel} = s_b$, $s_{\parallel} = s_{-b}$, which are passing through the intersection points of the line $z = 2Fs_A$ with the curves $z = a(s_{\parallel}) + b(s_{\parallel})$, $z = a(s_{\parallel})$, $z = b(s_{\parallel})$ and $z = -b(s_{\parallel})$, respectively. Inside the individual intervals along the s_{\parallel} axis the functions under the integral are approximated by the leading terms of their Taylor's expansion (assuming the validity of the strong inequalities of the type $a \gg |b| \gg 1$, $a \gg Fs_A$ or $a \ll Fs_A$, $b \gg Fs_A$ or $b \ll Fs_A$). Note, in particular, that strong inequality $a \gg |b| \gg 1$ holds (in the high amplitude regime $s_A \gg 1$ of interest) practically in the whole integration region. Because of this it is possible to approximate practically everywhere $a \approx \exp(s_A + s_{\parallel})/2$ and $b \approx \text{sign}(s_A - s_{\parallel}) \exp(|s_A - s_{\parallel}|)/2$.

The analysis has demonstrated, that three different frequency regimes can be identified. The high-frequency regime is determined by the inequality

$$F \gg F_H \equiv \exp(2s_A)/(4s_A). \quad (53)$$

In Fig. 7(a) the curves and the intersections points at the plane (s_{\parallel}, z) , which are important for this regime, are presented schematically. It has been found that the dominant contribution to stress $\bar{\sigma}$ is provided in this regime by the region $0 \leq s_{\parallel} \leq s_{a+b}$, $0 \leq z \leq a+b$ presented in gray color in Fig. 7(a). However, even this dominant contribution is very small

$$|\bar{\sigma}| \approx \frac{1}{4Fs_A} \frac{\ln[4Fs_A/\exp(2s_A)]}{[4Fs_A/\exp(2s_A)]} = \frac{1}{4Fs_A} \frac{\ln(F/F_H)}{(F/F_H)} \ll 1. \quad (54)$$

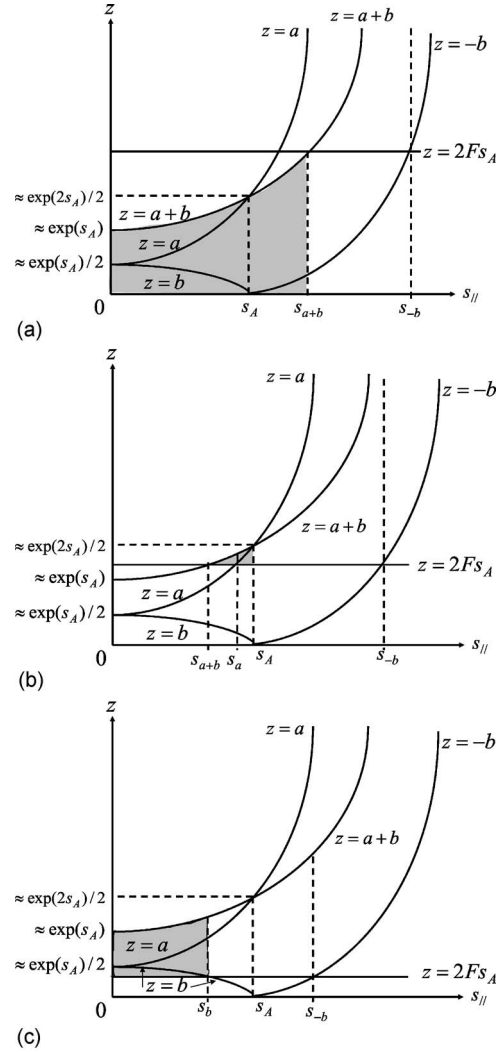


FIG. 7. Schematic presentation of the division of the integration domain ($0 \leq s_{\parallel} \leq \infty, 0 \leq z \leq a+b$) in subdomains for different regimes of acoustic loading. (a) High-frequency regime ($F \gg F_H$). (b) First intermediate frequency regime ($F_I \ll F \ll F_H$). (c) Second intermediate frequency regime ($F \ll F_I$).

The significant values of $\bar{\sigma}$ has been found only in the regimes where $s_{a+b} \leq s_A$. For the first of the intermediate frequency regimes

$$\exp(s_A)/(4s_A) \equiv F_I \ll F \ll F_H \equiv \exp(2s_A)/(4s_A), \quad (55)$$

the integration plane is presented in Fig. 7(b). It has been found that the dominant contribution to stress $\bar{\sigma}$ is provided in this regime by the region $s_a \leq s_{\parallel} \leq s_A$, $2Fs_A \leq z \leq a+b$ presented in gray color in Fig. 7(b). This contribution contains the dominant component, which is quadratic in strain

$$\bar{\sigma} \approx -4s_A^2 + [\ln(4Fs_A)]^2. \quad (56)$$

Note that, although for $F \ll F_H$ the inequality $4Fs_A \ll \exp(2s_A)$ holds, it does not ensure that in Eq. (56) the second corrective term is completely negligible. In particular, by retaining the second term, it is possible to predict correctly the tendency in stress diminishing when the frequency

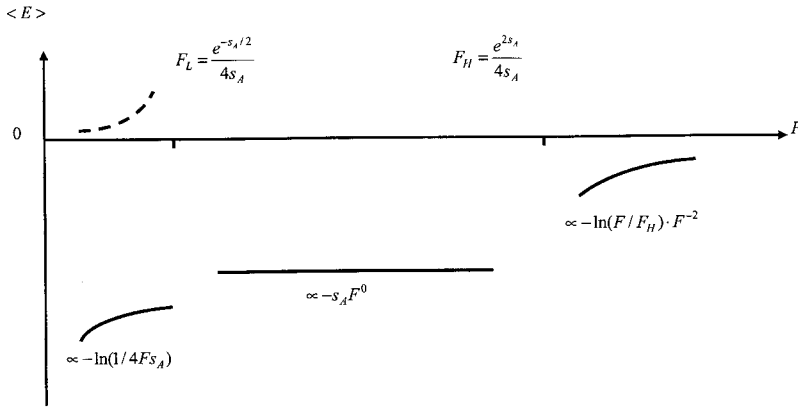


FIG. 8. Schematic illustration of the variation with frequency of the amplitude-dependent modulus defect $\langle E \rangle$ in the case of the high-amplitude acoustic loading.

F approaches the critical high frequency F_H . However, the dominant dependence of stress on the strain amplitude [when the amplitude varies in the limited range, ensuring that the frequency satisfies the inequality (55)] is clearly quadratic ($\bar{\sigma} \propto -s_A^2$).

The second of the intermediate frequency regimes has been found in the limit

$$F \ll F_I \equiv \exp(s_A)/(4s_A). \quad (57)$$

The integration plane is presented in Fig. 7(c). It has been found that the dominant contribution to stress $\bar{\sigma}$ is provided in this regime by the region $0 \leq s_{\parallel} \leq s_b$, $2Fs_A \leq z \leq a+b$ presented in gray color in Fig. 7(c),

$$\bar{\sigma} \approx -s_A^2 + 2s_A \ln(4Fs_A). \quad (58)$$

In Eq. (58) the contribution to stress, which is quadratic in strain, dominates in the range

$$\exp(-s_A/2)/(4s_A) \equiv F_L \ll F \ll F_I \equiv \exp(s_A)/(4s_A), \quad (59)$$

i.e., below the critical intermediate frequency F_I , but not too below. Quadratic dependence of stress on strain amplitude disappears in the low frequency regime defined by the inequality

$$F \ll F_L \equiv \exp(-s_A/2)/(4s_A). \quad (60)$$

In the low frequency regime (60) the dependence of stress on the strain amplitude is basically quasilinear

$$\bar{\sigma} \approx -2s_A \ln[1/(4Fs_A)]. \quad (61)$$

The results presented in Eqs. (53)–(61) correlate with the expectations. First, the Preisach-Mayergoyz regime [with $\sigma(s=s_A) \propto -s_A^2$, and, consequently, $\langle E \rangle \propto -s_A$] has been found. It is predicted that PM regime can be obtained for $s_A \gg 1$ in a wide frequency interval

$$\exp(-s_A/2)/(4s_A) \equiv F_L \ll F \ll F_H \equiv \exp(2s_A)/(4s_A). \quad (62)$$

Please note that for $s_A \gg 1$ we have $F_L \ll 1$, while $F_H \gg 1$, so the frequency interval in Eq. (62) is very large. In accordance with a schematic presentation in Fig. 8 the secant modulus in the considered case of high-amplitude acoustic loading diminishes with increasing frequency [compare to the case of

low-amplitude loading in Fig. 5(b)]. Please note that the contribution to $\langle E \rangle$ at low frequencies $F \ll F_L$ weakly (logarithmically) depends on the wave amplitude. In other words the basic contribution is amplitude-independent, while the amplitude-dependent contribution (presented by dashed curve in Fig. 8) grows in magnitude. Consequently the theory predicts that acoustic nonlinearity grows in magnitude with increasing frequency of high-amplitude excitation ($s_A \gg 1$) in the low frequency domain $F \ll F_L$, that it does not depend on frequency in the intermediate frequency domain $F_L \ll F \ll F_H$ of quadratic hysteretic nonlinearity, and that it falls in the high frequency domain $F \gg F_H$. In other words the acoustic nonlinearity falls outside the domain (62) of the approximate validity of the Preisach-Mayergoyz model of rate-independent zero-temperature hysteresis.

Second, in accordance with the derived formulas (61) and (58) in transition from the low frequency regime $F \ll F_L$ to the intermediate frequency regime $F_L \ll F \ll F_H$ the dominant contribution to maximum stress changes from linear in strain to quadratic in strain. So the critical frequency F_L can be identified as a transition frequency (for the material loaded by high amplitude acoustic waves) from the regime, where its elements behave (in average over their distribution) as quasiequilibrium ones (Fig. 3), to the regime, where they behave as bistable units (Fig. 1).

Third, in accordance with the derived formulas (56) and (54) in the transition from the intermediate frequency regime $F_L \ll F \ll F_H$ to the high frequency regime $F \gg F_H$ there is a significant fall in stress accompanied by the disappearance of the contribution, which is quadratic in strain amplitude (typical of PM model). Consequently, the critical frequency F_H can be identified as a transition frequency (for the material loaded by high amplitude acoustic waves) from the regime, where its elements behave (in average over their distribution) as bistable units, to the regime, where they behave as quasi-frozen ones. All three observations mentioned just above correlate with the expectations formulated in the beginning of this section.

In accordance with the obtained results, if the dominant contribution to the modulus defect in experiment is linear in wave amplitude, this necessitates the strong inequality $s_A \gg 1$. In other words the dimensional acoustic strain amplitude should significantly exceed the characteristic strain $s_0 = k_B T/d$ of the material. Then the theory predicts that the dispersion of the nonlinearity (accompanied by the deviation

from the $\langle E \rangle \propto -s_A$ law) might be expected in the frequency ranges $F \leq F_L$ and $F \geq F_H$.

It should be also noted that the obtained results correlate as well with the expected dependence of the modulus defect on the wave amplitude. For the analysis it should be taken into account, that in comparison with the low amplitude regime, where the dependence of the critical transition frequencies F_L and F_H on the wave amplitude is negligible (see Figs. 5 and 6), in the high amplitude regime the dependence of the critical frequencies on the wave amplitude is exponentially strong (see Fig. 8). For example, if for the initial amplitude of the acoustic excitation with $s_A \gg 1$ the system is in the low frequency regime $F \ll F_L$, then with increasing s_A the characteristic frequency $F_L \equiv \exp(-s_A/2)/(4s_A)$ diminishes and sooner or later the opposite condition $F_L \ll F$ will be fulfilled. This corresponds to the transition of the system with increasing wave amplitude from the low-frequency quasilinear regime (61) to the intermediate frequency regime characterized by $\bar{\sigma} \propto -s_A^2$ (58) typical of PM model.

If for the initial amplitude of the acoustic excitation with $s_A \gg 1$ the system is in the high frequency regime $F \gg F_H$, then with increasing s_A the characteristic frequency $F_H \equiv \exp(2s_A)/(4s_A)$ increases and sooner or later the opposite condition $F \ll F_H$ will be fulfilled. This corresponds to the transition of the system with increasing wave amplitude from the high-frequency quasifrozen regime (54) to the intermediate frequency regime characterized by $\bar{\sigma} \propto -s_A^2$ (56) typical of PM model.

VII. DISCUSSION

The general conclusion from the analysis undertaken in Secs. III–V is the following. In the Preisach-Arrhenius system of hysteretic mechanical elements, subjected to low amplitude acoustic loading with $s_A \ll 1$, significant frequency dispersion of both elastic and inelastic (of both linear and nonlinear) properties is expected only outside a broad frequency interval $\exp(-s_A^{\max}) \ll \pi F \ll 1$. The prediction of the wide frequency range, where the decrement is frequency independent and linear wave velocity scales as logarithm of frequency, is in accordance with multiple experimental observations.^{33,36} It should be mentioned here that almost constant acoustic decrement is known to be associated with the logarithmic creep,^{43,44} which is also frequently observed in rocks. Because of this the derived above prediction of constant decrement could have been expected in view of the fact that the logarithmic in time dynamics of the flux creep had been recently predicted for magnetics on the basis of the Preisach-Arrhenius model.^{24,25} The question is how the theoretical prediction of frequency-independent decrement depends on the simplifying assumptions accepted for the evaluation of the PA model? Additional analysis has demonstrated that the essential point is the assumption of the flat distribution of $\Delta\sigma'f$ near the diagonal of the PM space, i.e., near the $\sqrt{2}s_{\parallel}$ axis (see Fig. 2). It is straightforward to verify that, if any distribution (descending with increasing s_{\perp}) is added in the region $s_{\perp} \geq s_{\perp}^{\max}$ to the assumed above “rectangular” distribution of $\Delta\sigma'f$ in Fig. 2, then the asymptotic behavior of acoustic properties in the interval $\exp(-s_{\perp}^{\max}) \ll \pi F \ll 1$ will

not be modified. From a physics point of view this is due to the fact that the relaxation frequency of the elements depends exponentially on s_{\perp} [see Eq. (11)]. For the frequencies in the range $\exp(-s_{\perp}^{\max}) \ll \pi F \ll 1$ the elements of the PM space, which are located at the distances $s_{\perp} \geq s_{\perp}^{\max}$, even if they exist there, are quasifrozen and, as a consequence, they provide very small contribution to the acoustic properties. The distribution of the mechanical elements in the region $s_{\perp} \geq s_{\perp}^{\max}$, however, influences the frequency dependence of the acoustic properties in the domain $\pi F \leq \exp(-s_{\perp}^{\max})$.

Another interesting theoretical result for low amplitude acoustic loading with $s_A \ll 1$ is the prediction of the transition from the nonlinear induced transparency at low frequencies to nonlinear induced absorption at high frequencies. It is tentative to attribute this effect in full to the nonlinear shift of the relaxation frequencies of the elements with increasing wave amplitude. In fact from Eq. (30) it follows that the resonance frequency of the elements increases in average over the wave period with increasing wave amplitude. The corresponding shift of the resonance curve in Fig. 5(a) (obtained for the case of the linear absorption) to higher frequencies naturally explains the nonlinear transparency below the resonance peak and nonlinear absorption above the resonance peak [see Fig. 6(a)]. However the nonlinear effects in the considered system are not only due to the dependence of the relaxation frequencies on acoustic excitation [the coefficient $1/\tau_{12} + 1/\tau_{21}$ in Eq. (6)]. The driving term ($1/\tau_{21} - 1/\tau_{12}$) in Eq. (6), which is due to the asymmetry of the transitions between the states, also depends on the amplitude of the acoustic excitation. Consequently the explanation based on the shift of the resonance, proposed just above, is only a qualitative guideline for the intuitive understanding of the predicted phenomenon.

In accordance with Sec. VI in the case of the high amplitude acoustic loading ($s_A \gg 1$) the dispersion of the material properties is expected (similar to the low-amplitude case $s_A \ll 1$) only outside of a broad frequency interval $\exp(-s_A/2)/(4s_A) \equiv F_L \ll F \ll F_H \equiv \exp(2s_A)/(4s_A)$. However in the considered high amplitude regime (in contrast to the low-amplitude regime $s_A \ll 1$) the characteristic boundary frequencies of this interval F_L and F_H importantly depend on the wave amplitude. Inside the above mentioned interval the regime of hysteretic quadratic nonlinearity (PM regime) with $\sigma(s=s_A) \propto -s_A^2$ and $\langle E \rangle \propto -s_A$ is realized. In the low amplitude regime ($s_A \ll 1$) the theory developed in Sec. V predicts that the lowest amplitude-dependent contribution to the modulus defect $\langle E^{(3)} \rangle$ will be quadratic in wave amplitude [$\langle E^{(3)} \rangle \propto s_A^2$ due to Eq. (42)] at all possible frequencies. Consequently the developed theory predicts the possibility of the transition from the law $\langle E^{(3)} \rangle \propto s_A^2$ (typical of cubic nonlinearity) to the law $\langle E \rangle \propto -s_A$ (typical of hysteretic quadratic nonlinearity) with acoustic amplitude increasing from $s_A \ll 1$ to $s_A \gg 1$. This transition is expected to proceed differently at different frequencies. When the characteristic frequencies F_L and F_H are estimated for $s_A \approx 1$ as $F_L(s_A \approx 1) \approx 0.4$ and $F_H(s_A \approx 1) \approx 1.9$, respectively, then it becomes clear that $F_L(s_A \approx 1) < F_H(s_A \approx 1)$ and three different scenarios are possible. At frequencies $F \leq F_L(s_A \approx 1)$ the transition takes place through the intermediate low frequency high amplitude re-

gime (60) and (61). The dominance of the quadratic nonlinearity is expected for the acoustic amplitudes satisfying the inequality $F_L(s_A) \equiv \exp(-s_A/2)/(4s_A) \leq F$, when the system shifts with increasing wave amplitude from the low frequency regime (60) and (61) to the intermediate frequency regime (58) and (59). For $F_L(s_A \approx 1) \leq F \leq F_H(s_A \approx 1)$ the transition is direct and takes place at $s_A \propto 1$. For $F_H(s_A \approx 1) \leq F$ the transition takes place through the intermediate high frequency regime (53) and (54). The dominance of the quadratic nonlinearity is expected for the acoustic amplitudes satisfying the inequality $F \leq \exp(2s_A)/(4s_A) \equiv F_H(s_A)$, when the system shifts with increasing wave amplitude from the high frequency regime (53) and (54) to the intermediate frequency regime (55) and (56).

From the previous paragraph it follows that the PA model of acoustic nonlinearity does explain the experimentally observed^{18–20} low-amplitude threshold for the transition to hysteretic quadratic nonlinearity with increasing wave amplitude. Importantly the theory predicts the conditions for the transition ($F_L=F$ or $F_H=F$). Consequently when the threshold strain amplitude, at which the transition to $\langle E \rangle \propto -s_A$ takes place, is found experimentally then the condition $F_L=F$ (or $F_H=F$) provides the relation between the attempt time τ_0 and the deformation potential d in the material. This relation might be used in the future to check the microscopic theories developed for the evaluation of τ_0 and d , when they are available. Currently, in view of the existing consensus on the values of the attempt frequency [$O(10^8-10^{12}$ Hz)] it is possible from the experimental data^{18–20} to estimate the deformation potentials. For example, the nondimensional frequency in the experiment¹⁹ conducted at 39 kHz can be estimated as $F \propto \tau_0/T \propto 4(10^{-4}-10^{-8}) \ll 1$. Consequently, in the frame of the theory developed above, the transition is taking place through the intermediate high amplitude low frequency regime (60) and (61) and it finishes when $s_A \geq (8.6-25)s_0$. In experiment¹⁹ the transition has been found around $s_A \approx 2 \times 10^{-7}$. Comparison of the theory and the experiment provides an estimate of the characteristic strain $s_0 \propto (2-1) \times 10^{-8}$ and of the deformation potential $d = k_B T / s_0 \propto (1.3-2.6)$ MeV. Important conclusion from these estimates is the following. Due to low (kHz) frequencies of the excitation the transition is observed not at the acoustic strains of the order of the characteristic one, but at an order of magnitude larger strains. This made the observations possible. The characteristic strain s_0 itself is very small. In the experiments²⁰ conducted at even lower frequencies in comparison with Ref. 19 the experimentally determined threshold strain for the transition was higher. This trend is in accordance with the theoretical predictions that at lower frequencies higher acoustic amplitudes are necessary to overcome the influence of thermal fluctuations, which are destroying hysteresis. However the possible difference in the deformation potentials of the single crystal¹⁹ and polycrystalline metals²⁰ should be taken into account in quantitative comparison. In rocks the observation of the transition from $\langle E^{(3)} \rangle \propto -s_A^2$ to $\langle E \rangle \propto -s_A$ has been reported at strain around 10^{-6} at frequencies as low as 0.5–3 kHz.¹⁸ The estimates using these data indicate that for the mesoscopic mechanical elements in rocks the characteristic strain s_0 is about 3 times

larger and the deformation potential is about 3 times smaller than for the dislocations in single crystal metals. Note that in both experiments^{18,19} the transition to $\langle E \rangle \propto -s_A$ was detected for the acoustic strain amplitudes which are close to ultimate sensitivity of the detection system. So the data from these experiments cannot be used to compare with the predictions from the developed theory in a wide enough interval starting from $s_A \rightarrow 0$ and finishing with $s_A \rightarrow \infty$. Unfortunately below the transition the experimental data are available only in a rather narrow amplitude band. However, as it has been demonstrated above, just the observation of the transition can be used to estimate some parameters of the micromechanical elements. Note that the recent experiments⁴⁵ has confirmed once again that the contribution of the rate-independent hysteresis to the nonlinearity of geomaterials can be negligible at sufficiently low acoustic strain amplitudes.

Finally, it should be clearly stated that the thermal relaxation Preisach-Arrhenius model does not include all the effects producing rate-dependence of the hysteresis. See, for comparison, the description of rate-dependent hysteretic phenomena in magnetism.¹³ For example the rate-dependence should also appear due to the fact that acoustic field cannot, in principle, transform mechanical elements from one configuration (state) to another infinitely fast.^{13,15} In other words an individual mechanical element cannot change its configuration instantaneously either due to direct effect of the acoustic field or due to thermal fluctuations. In Preisach-Arrhenius model the finite transition time appears only statistically in averaging over all the elements, while each of the elements still exhibits instantaneous transitions as in the zero-temperature (PM) model. To introduce finite transition times for the individual elements a micromechanical model of the transition between the different states (configurations) should be formulated (see, for example, Refs. 13 and 46) or the finite transition times can be introduced phenomenologically as a temperature-independent relaxation process.¹⁵ Surely the generalized theoretical model of hysteresis should include correct description of the temporal dynamics of both the transitions caused by thermal fluctuations and directly by the acoustic forces. The development of a generalized model would be highly desirable for the explanation of the recent experiments,^{20,47,48} where the dependence of the acoustic nonlinearity of the mesoscopic materials on frequency has been documented.

VIII. CONCLUSIONS

The analytical evaluation of the Preisach-Arrhenius model for the acoustic hysteresis given here demonstrates that thermal effects are capable of inducing dispersion in both the linear and nonlinear acoustic properties of microinhomogeneous materials. Thermal effects can also induce important deviations in the amplitude-dependent behavior of the material from one predicted by the Preisach-Mayergoyz (zero-temperature) model. The theory predicts the boundaries for an intermediate interval of frequencies where hysteretic quadratic nonlinearity dominates in a mesoscopic material at sufficiently high amplitudes of acoustic excitation. Outside of this interval (at sufficiently low or sufficiently high fre-

quencies) the nonlinearity deviates from one predicted by the Preisach-Mayergoyz model and diminishes. However the width of the frequency interval for the hysteretic quadratic nonlinearity depends on the wave amplitude and broadens with the increasing wave amplitude. The low-frequency cut-off of the interval diminishes with increasing wave amplitude while the high-frequency cutoff increases. As a result, if at sufficiently low acoustic amplitudes the system manifests a quasilinear nonlinearity it will, with increasing

wave amplitude, sooner or later manifest a hysteretic quadratic nonlinearity. Thus the Preisach-Arrhenius model of acoustic hysteresis explains the transition in acoustic behavior of microinhomogeneous materials from one characterized by dominance of the quasilinear nonlinearity to another characterized by dominance of the hysteretic quadratic nonlinearity. This transition has been observed with increasing wave amplitude in a number of microinhomogeneous materials.

*Electronic address: vitali.goussev@univ-lemans.fr; Phone: +33 2 43 83 39 76; Fax: +33 2 43 83 35 18

¹V. E. Nazarov, L. A. Ostrovsky, I. A. Soustova, and A. M. Sutin, *Phys. Earth Planet. Inter.* **50**, 65 (1988).

²V. E. Nazarov, L. A. Ostrovsky, I. A. Soustova, and A. M. Sutin, *Akust. Zh.* **34**, 491 (1988) [*Sov. Phys. Acoust.* **34**, 284 (1988)].

³R. A. Guyer and P. A. Johnson, *Phys. Today* **52**, 30 (1999).

⁴R. A. Guyer, J. TenCate, and P. Johnson, *Phys. Rev. Lett.* **82**, 3280 (1999).

⁵L. D. Landau and E. M. Lifshitz, *Theory of Elasticity* (Pergamon, London, 1959).

⁶L. V. Zarembo and V. A. Krasilnikov, *Usp. Fiz. Nauk* **102**, 549 (1970) [*Sov. Phys. Usp.* **13**, 778 (1971)].

⁷V. E. Nazarov, *Akust. Zh.* **47**, 509 (2001) [*Acoust. Phys.* **47**, 438 (2001)].

⁸S. Asano, *J. Phys. Soc. Jpn.* **29**, 952 (1970).

⁹I. D. Mayergoyz, *Mathematical Models of Hysteresis* (Springer-Verlag, Berlin, 1992).

¹⁰D. J. Holcomb, *J. Geophys. Res.* **86**, 6235 (1981).

¹¹R. A. Guyer, K. R. McCall, and G. N. Boitnott, *Phys. Rev. Lett.* **74**, 3491 (1995).

¹²M. A. Krasnosel'skii and A. V. Pokrovskii, *Systems with Hysteresis* (Springer-Verlag, Berlin, 1989).

¹³G. Bertotti, *Hysteresis in Magnetism* (Academic, San Diego, 1998).

¹⁴V. E. Gusev, C. Glorieux, W. Lauriks, and J. Thoen, *Phys. Lett. A* **232**, 77 (1997).

¹⁵V. E. Gusev, W. Lauriks, and J. Thoen, *J. Acoust. Soc. Am.* **103**, 3216 (1998).

¹⁶V. Aleshin, V. Gusev, and V. Zaitsev, *J. Comput. Acoust.* **12**, 319 (2004).

¹⁷V. E. Gusev, *Wave Motion* **33**, 145 (2001).

¹⁸J. A. TenCate, (private communication).

¹⁹A. S. Nowick, *Phys. Rev.* **80**, 249 (1950).

²⁰V. E. Nazarov, A. V. Radostin, and I. A. Soustova, *Akust. Zh.* **48**, 85 (2002) [*Acoust. Phys.* **48**, 76 (2002)].

²¹E. Della Torre, *Magnetic Hysteresis* (IEEE, New York, 1999).

²²E. Della Torre, *IEEE Trans. Magn.* **34**, 1276 (1998).

²³O. Alejos and E. Della Torre, *IEEE Trans. Magn.* **37**, 3345 (2001).

²⁴G. Bertotti, *Phys. Rev. Lett.* **76**, 1739 (1996).

²⁵V. Basso, C. Beatrice, M. LoBue, P. Tiberto, and G. Bertotti, *Phys. Rev. B* **61**, 1278 (2000).

²⁶A. V. Granato and K. Lücke, in *Physical Acoustics*, edited by W. P. Mason (Academic, New York, 1966), Vol. IV-A, p. 225.

²⁷L. J. Teutonico, A. V. Granato, and K. Lücke, *J. Appl. Phys.* **35**, 220 (1964).

²⁸*Handbook of Micro/Nano Tribology*, edited by B. Bhushan (CRC Press, Boca Raton, 1999), Chaps. 5 and 9.

²⁹*Physical Acoustics, Principles and Methods*, edited by W. P. Mason (Academic, New York, 1966), Vol. III, Part A.

³⁰R. A. Guyer, K. R. McCall, G. N. Boitnott, L. B. Hillbert, Jr., and T. J. Plona, *J. Geophys. Res.*, [Solid Earth] **102-B3**, 5281 (1997).

³¹V. Gusev and V. Aleshin, *J. Acoust. Soc. Am.* **112**, 2666 (2002).

³²E. Riedo, E. Gnecco, R. Bennewitz, E. Meyer, and H. Brune, *Phys. Rev. Lett.* **91**, 084502 (2003).

³³L. Knopoff, *Rev. Mod. Phys.* **30**, 1178 (1958).

³⁴L. Knopoff, in *Physical Acoustics*, edited by W. P. Mason (Academic, New York, 1965), Vol. III-B, Chap. 7.

³⁵J. Duffy and R. D. Mindlin, *Trans. ASME* **79**, 585 (1957).

³⁶M. J. Buckingham, *J. Acoust. Soc. Am.* **108**, 2796 (2000).

³⁷J. C. Savage, *J. Geophys. Res.* **71**, 3929 (1966).

³⁸G. M. Lundquist and V. C. Cormier, *J. Geophys. Res.* **85**, 5244 (1980).

³⁹I. A. Chaban, *Akust. Zh.* **39**, 362 (1993) [*Acoust. Phys.* **39**, 190 (1993)].

⁴⁰M. J. Buckingham, *J. Acoust. Soc. Am.* **102**, 2579 (1997).

⁴¹V. Yu. Zaitsev, V. E. Nazarov, *Akust. Zh.* **45**, 622 (1999) [*Acoust. Phys.* **45**, 522 (1999)].

⁴²A. B. Lebedev, *Phys. Solid State* **41**, 1105 (1999).

⁴³C. Lomnitz, *J. Geophys. Res.* **67**, 365 (1962).

⁴⁴E. Strick, *J. Geophys. Res.*, [Solid Earth] **89-B1**, 437 (1984).

⁴⁵J. A. TenCate, D. Pasqualini, S. Habib, K. Heitmann, D. Higdon, and P. A. Johnson, *Phys. Rev. Lett.* **93**, 065501 (2004).

⁴⁶B. Capogrosso-Sansone and R. A. Guyer, *Phys. Rev. B* **66**, 224101 (2002).

⁴⁷J. K. Na and M. A. Breazeale, *J. Acoust. Soc. Am.* **95**, 3213 (1994).

⁴⁸V. E. Nazarov, *Akust. Zh.* **46**, 228 (2000) [*Acoust. Phys.* **46**, 186 (2000)].